# UTILIZATION OF FLUIDIZED BED COMBUSTION ASHES AS RAW MATERIAL IN THE PRODUCTION OF A SPECIAL CEMENT

A THESIS SUBMITTED TO
THE GRADUATE SCHOOL OF NATURAL AND APPLIED SCIENCE
OF
MIDDLE EAST TECHNICAL UNIVERSITY

BY

İLKER SONER

IN PARTIAL FULFILLMENT OF THE REQUIREMENTS
FOR
THE DEGREE OF MASTER OF SCIENCE
IN
CHEMICAL ENGINEERING

JUNE 2009

Approval of the thesis:

**UTILIZATION OF FLUIDIZED BED COMBUSTION ASHES AS RAW MATERIAL IN THE PRODUCTION OF A SPECIAL CEMENT**

submitted by **İLKER SONER** in partial fulfillment of the requirements for the degree of **Master of Science in Chemical Engineering Department, Middle East Technical University** by,

Prof. Dr. Canan Özgen _____
Dean, Graduate School of Natural and Applied Sciences

Prof. Dr. Gürkan Karakaş _____
Head of Department, Chemical Engineering

Prof. Dr. Nevin Selçuk _____
Supervisor, Chemical Engineering Dept., METU

Prof. Dr. Ekrem Selçuk _____
Co-Supervisor, Metallurgical and Materials Engineering Dept., METU

**Examining Committee Members:**

Prof. Dr. Mustafa Tokyay _____
Civil Engineering Dept., METU

Prof. Dr. Nevin Selçuk _____
Chemical Engineering Dept., METU

Assist. Prof. Dr. Görkem Külah _____
Chemical Engineering Dept., METU

Dr. Aykan Batu _____
Business Development Manager, Mimag-Samko

Mehmet Kürkçü _____
Energy Expert, Energy Market Regulatory Authority

**Date:** 30.06.2009

**I hereby declare that all information in this document has been obtained and presented in accordance with academic rules and ethical conduct. I also declare that, as required by these rules and conduct, I have fully cited and referenced all material and results that are not original to this work.**

Name, Lastname: İlker SONER

Signature:

# ABSTRACT


UTILIZATION OF FLUIDIZED BED COMBUSTION ASHES
AS RAW MATERIAL IN THE PRODUCTION OF A SPECIAL CEMENT

Soner, İlker

M.Sc., Department of Chemical Engineering

Supervisor: Prof. Dr. Nevin Selçuk

Co-supervisor: Prof. Dr. Ekrem Selçuk

June 2009, 77 pages

Fluidized bed combustion (FBC) ashes containing significant amount of free CaO and $CaSO_4$ in addition to valuable inorganic acidic oxide ingredients such as $SiO_2$, $Fe_2O_3$ and $Al_2O_3$ can be utilized as potential raw materials in the production of non-expansive belite-rich calcium sulfoaluminate cement which is one of the special cement type of sulfoaluminate-belite cements having performance characteristics similar to those of ordinary portland cement besides lower energy requirements and $CO_2$ emissions during manufacturing.

Therefore, in this thesis study, possibility of producing non-expansive belite-rich calcium sulfoaluminate cement by adding FBC ashes in various proportions to the raw meal was investigated. For this purpose, a raw meal composed a mixture of limestone, bauxite, gypsum together with 10 wt % bottom ash and 15 wt % baghouse filter ash was prepared. It was sintered in a laboratory scale muffle furnace at temperatures of 1200, 1250 and 1300 °C for various holding times. The results of

chemical and mineralogical analysis as well as microscopic examination reveal that FBC ashes have the potential to be used in the raw meal due to the presence of characteristic mineral phases of this type of cements, i.e. yeelimite, larnite, ferrite and anhydrite, in the sample obtained at optimum sintering temperature of 1250 °C for 60 min.

**Keywords:** Ash utilization, fluidized bed combustion and energy saving cements

# ÖZ

AKIŞKAN YATAKLI YAKICI KAYNAKLI KÜLLERİN ÖZEL
BİR ÇİMENTO ÜRETİMİNDE HAMMADDE OLARAK KULLANILMASI

Soner, İlker
Yüksek Lisans, Kimya Mühendisliği Bölümü
Tez Yöneticisi: Prof. Dr. Nevin Selçuk
Ortak Tez Yöneticisi: Prof. Dr. Ekrem Selçuk

Haziran 2009, 77 sayfa

Asidik oksit içeriğine ek olarak önemli miktarda serbest CaO ve $CaSO_4$ içeren akışkan yataklı kazan külleri Portland çimentosu ile benzer performans özelliklerine sahip olmasının yanında üretimi esnasında enerji tasarrufu sağlayan ve atmosfere daha az $CO_2$ salan özel bir sülfo alümino-belit çimentosu olan genleşmesi düşük belitce zengin kalsiyum sülfo alümino çimentosu üretiminde hammadde olarak kullanılma potansiyeline sahiptirler.

Dolayısıyla, bu tez çalışmasında, hammadde karışımına belirli oranlarda akışkan yataklı kazan küllerinin eklenmesiyle genleşmesi düşük belitce zengin kalsiyum sülfo alümine çimentosunun üretim potansiyeli incelenmiştir. Bu amaçla, kireçtaşı, boksit, alçıtaşı ile ağırlıkça yüzde 10 taban külü ve yüzde 15 toz filtre külü içeren bir hammadde karışmı hazırlandı. Bu karışım laboratuar ölçekli bir fırında 1200, 1250 ve 1300 °C sıcaklıklarında değişik sürelerde tutularak sinterleştirilmiştir. Kimyasal,

mineralojik ve mikroskopik incelemeler sonucunda ideal sıcaklık olan 1250 °C'de 60 dakika süreyle bekletilen örnekteki bu tür çimentolara ait karakteristik mineral fazların görülmesi dolayısıyla akışkan yataklı kazan küllerinin hammadde karışımında kullanım potansiyeline sahip olduğu anlaşılmıştır.

**Anahtar Kelimeler:** Kül değerlendirme, akışkan yataklı yakma teknolojisi ve enerji tasarruflu çimentolar

*To My Parents*

# ACKNOWLEDGMENTS

I would like to express my sincere gratitude to my supervisor, Prof. Dr. Nevin Selçuk for her enthusiastic supervision, insightful conversations during the development of this thesis, and helpful comments on the text. I would like to extend my appreciation to my co-supervisor Prof. Dr. Ekrem Selçuk, for his precious suggestions and support.

I am very grateful for the technical assistance provided by Kerime Güney for chemical analysis; Yusuf Yıldırım for heat treatment applications; Necmi Avcı for XRD analysis and Cengiz Tan for SEM/EDX analysis.

Financial support provided by Middle East Technical University (METU) through BAP-2006.07.02.00.01 project is gratefully acknowledged.

My very special thanks go to my family for their great support, encouragement and unshakable faith in me.

# TABLE OF CONTENTS

# LIST OF TABLES

**TABLES**

# LIST OF FIGURES

**FIGURES**

# ABBREVIATIONS

**ABFBC** Atmospheric Bubbling Fluidized Bed Combustion

**CCBs** Coal Combustion Byproducts

**CFBC** Circulating Fluidized Bed Combustion

**DTA** Differential Thermal Analysis

**EDS** Energy Dispersive Spectrometer

**FBC** Fluidized Bed Combustion

**FGD** Flue Gas Desulphurization

**JCPDS** Joint Committee on Powder Diffraction Standards

**LOI** Loss on Ignition

**MW** Molecular Weight

**OPC** Ordinary Portland Cement

**PC** Portland Cement

**PPC** Pulverized Coal Combustion

**SAB** Sulfoaluminate Belite

**SEM** Scanning Electron Microscopy

**TGA** Thermal Gravimetric Analysis

**Cement Chemical Notation**

| | |
|---|---|
| **C** | CaO |
| **S** | $SiO_2$ |
| **A** | $Al_2O_3$ |
| **F** | $Fe_2O_3$ |
| $\overline{\mathbf{S}}$ | $SO_3$ |
| **H** | $H_2O$ |

# CHAPTER 1

# INTRODUCTION

## 1.1 General

Coal is the leading fossil fuel with 826 billion tons of estimated recoverable reserves spreading worldwide. It provides 26 % of global primary energy needs and generates 41 % of the world's electricity [1, 2]. Fluidized bed combustion (FBC) of coal for power generation is a steadily increasing clean combustion technology in both capacity and number due to so many advantages like higher fuel flexibility, higher combustion efficiency, lower combustion temperatures (usually in the range of 750-950 °C) and lower emissions over conventional pulverized coal combustion technology with no post treatment equipment for flue gases [3, 4]. Consumption of coal for electricity generation leads to excess amount of coal combustion by-products (CCBs) which are a combination of noncombustible inorganic residue and incompletely combusted organics [5].

Fluidized bed combustors generate mainly two streams of CCBs as fly ash and bottom ash. Fly ashes are the fine particles carried away by the flue gas and collected in a bag filter or electrostatic precipitator whereas bottom ashes are the coarse spent materials removed from the bottom of the furnace. Both ashes contain same type of minerals but in different proportions [6, 7]. Regarding the chemical composition of FBC ashes containing valuable inorganic compounds like oxides of silicon, aluminum, calcium and iron, they can be considered as suitable raw materials in the production of cement. However, their high sulfate, free lime and

unburnt carbon contents together with poor pozzolanic activity due to the reduced glass content related to lower combustion temperatures restrain their use in the Portland cement and concrete industry. Therefore, other type of special cements based at least in part on calcium sulfates may provide a way to utilize these ashes in the raw meal [8-14].

In recent years, sulfoaluminate-belite (SAB) cement which is one of the special cements has drawn more attention compared to ordinary Portland cement (OPC) due to their following advantages [13, 16-18]:

- Reduced energy consumption during manufacturing due to lower lime contents of its major components which are formed at temperatures around 1200 – 1300 °C as opposed to around 1450 °C resulting in about 16 % energy saving and to 25 % lower grinding energy owing to relatively soft and friable nature of its clinker [15, 19-23].
- Low $CO_2$ emissions during manufacturing due to reduction in limestone utilization resulting in up to 40 % less $CO_2$ emissions. Total lime requirement of SAB cements is about 50 wt %, that is, 15 percentage points less than OPC [19, 20, 24].
- Low $NO_x$ emissions during manufacturing owing to lower clinkerization temperatures [15].
- Reduction in consumption of natural resources by substituting a variety of industrial by-products such as fly ash, blast furnace slag, FGD waste etc. as raw materials [9, 25, 26].
- Use of lower carbonate content limestone as natural raw material is feasible [15].
- High resistance to sulfate attack since their phases are fully sulfated [27].

Consequently, this binder can give a substantial contribution to the saving of natural resources, energy and environment.

Industrial wastes high in sulfate content can be a valuable source as raw materials in the production of SAB cement since this special cement contains inherently two sulfate-rich phases as calcium sulfoaluminate and calcium sulfate instead of tricalcium silicate and tricalcium aluminate phases of OPC [20,22,23,28-30]. Therefore, ashes generated from fluidized bed combustion of low calorific value, high ash and sulfur content Turkish lignites containing high CaO and $SO_3$ besides their higher acidic oxide contents have significant potential to be utilized as raw materials in the production of SAB cement. Non-expansive belite-rich calcium sulfoaluminate type of SAB cement having higher belite and lower calcium sulfoaluminate contents than commercially produced calcium sulfoaluminate-rich belite cement has both physical and mechanical properties comparable to OPC [13,15,17,26,29,30].

## 1.2 Aim and Scope of the Thesis

Steady increase in the applications of environmentally clean fluidized bed combustion technology in both number and capacity over the past decade has led to the investigation of the possibilities for utilization of FBC ashes. Furthermore, the pressure to reduce both energy consumption and $CO_2$ emissions during manufacture of OPC has been major factors contributing to the development of special cements.

Therefore, the objective of this thesis study is to produce energy efficient and high value added non- expansive belite-rich calcium sulfoaluminate cement at laboratory scale by utilizing FBC ashes at suitable proportions in the cement raw meal and to investigate the synthesized cement with respect to its chemical and mineral composition.

# CHAPTER 2

# BACKGROUND AND LITERATURE REVIEW

## 2.1 General

Prior to presenting a detail review of previous studies on the laboratory scale production of calcium sulfoaluminate based cements, various issues associated with the Ordinary Portland Cement (OPC) which is currently the most commonly used type of cement in the world and sulfoaluminate-belite cement (SAB) which is one of the special cements under investigation owing to their significant environmental advantages with energy savings during manufacturing and potential use of fluidized bed combustion (FBC) ashes as raw materials are overviewed.

## 2.2 Ordinary Portland Cement

### 2.2.1 General

Ordinary Portland cement (OPC) as a hydraulic binder produced by grinding 3 – 5 % gypsum together with OPC clinker, which is an intermediate product and manufactured by sintering a proportioned mixture of calcareous materials (limestone, marl, chalk etc.) and argillaceous materials (clay, shale, slate etc.) [31-33].

Portland cement (PC) industry consumes a vast amount of energy and generates large amounts of $CO_2$ emissions during manufacturing process. Energy is required for the sintering of the high lime content of raw meal to form the characteristic

mineral compounds of PC clinker at high temperatures of around 1450 °C and for the grinding of the obtained rigid clinkers into cements with additives. Pulverized coal is generally used to provide the required energy and as expected combustion of coal increases the $CO_2$ emissions. Furthermore, limestone is the principle raw material used in the production of PC clinker and calcination reaction releases

$$CaCO_3 \longrightarrow CaO + CO_2 \qquad (2.1)$$

excessive volumes of $CO_2$ into the atmosphere according to reaction in equation (2.1). The raw materials of cement also require quarrying or mining operations which are energy intensive and environmentally undesired processes. Utilization of wastes including sulfates, which are increasing widespread due to the implementation of sulfur dioxide emission controls, in the production of OPC are restricted with the limitations on the sulfate content of cement with various standards. On the other hand, technical constraints of the OPC together with consumer confidence make it difficult to challenge their dominance [27].

### 2.2.2 Chemical and Mineralogical Composition

The four principle mineral phases of the OPC with their common names, chemical formulae and abbreviated notations are summarized in Table 2.1.

**Table 2.1:** Major mineral phases of OPC

| | **Tricalcium Silicate** | **Dicalcium Silicate** | **Tricalcium Aluminate** | **Tetracalcium Aluminoferrite** |
|---|---|---|---|---|
| **Common Name** | Alite | Belite | Aluminate | Ferrite |
| **Formulae** | $3CaO.SiO_2$ | $2CaO.SiO_2$ | $3CaO.Al_2O_3$ | $4CaO.Al_2O_3.Fe_2O_3$ |
| **Abbreviation** | $C_3S$ | $C_2S$ | $C_3A$ | $C_4AF$ |

Average chemical composition and corresponding potential Bogue composition for a typical OPC are given in Table 2.2 and Table 2.3, respectively. The following abbreviated chemical notation is used throughout the text:

C = CaO, S = $SiO_2$, A = $Al_2O_3$, F = $Fe_2O_3$, $\overline{S}$ = $SO_3$, H = $H_2O$,

**Table 2.2:** Average chemical composition of a typical OPC, wt % [34]

| Components | OPC |
|---|---|
| **LOI** | 1.125 |
| **CaO** | 64.783 |
| **$SiO_2$** | 20.783 |
| **$Al_2O_3$** | 4.900 |
| **$Fe_2O_3$** | 2.467 |
| **$SO_3$** | 2.750 |
| **MgO** | 1.250 |
| **$K_2O$** | 0.653 |
| **$Na_2O$** | 0.175 |
| **Rest** | 1.113 |
| **Total** | 100.000 |

**Table 2.3:** Potential Bogue mineral compositions of a typical OPC, wt% [34]

| Mineral Phases | OPC |
|---|---|
| **$C_3S$** | 55.667 |
| **$C_2S$** | 17.500 |
| **$C_3A$** | 8.800 |
| **$C_4AF$** | 7.500 |

The lime content of cement around 65 % is necessary due to the presence of high lime compounds such as $C_3S$ and $C_3A$ in the structure of OPC.

The relative proportions of these minerals affect the final properties of the cement. These compounds have the following specific properties [35-37]:

**Tricalcium Silicate:** The $C_3S$ is a solid solution forming around 55 – 65 % of the PC clinker, and is called as alite due to incorporation of some foreign oxides like MgO, $Al_2O_3$, $Fe_2O_3$, and $TiO_2$. It is composed of monoclinic or trigonal forms in the clinker. It is the major and most desired hydraulic calcium silicate of the OPC, providing early strength and rapid hardening of the cement paste. This compound requires the greatest amount of CaO and high sintering temperatures for its formation.

**Dicalcium Silicate:** Chemically pure $C_2S$ is also not present in the PC clinker and it is called as belite which has a content of 15 – 20 % of the PC clinker. Five polymorphic forms, α, $\alpha'_H$, $\alpha'_L$, β and γ, of $C_2S$ are known whereas predominantly the β form with a monoclinic unit cell exists in PC clinker. Its strength development is slow but it attains the same strength of alite at later ages.

**Tricalcium Aluminate:** The $C_3A$ content in PC clinker is approximately 4 – 11 % and it is the most reactive compound of the cement and liberates a significant amount of heat during the first few days of hydration. In order to retard the rapid reaction of this phase with water and hence to prevent a sudden loss of plasticity (*flash set*) of the cement paste, clinker should be ground with some source of sulphate addition, generally in the form of gypsum.

**Tetracalcium Aluminoferrite:** A solid solution of compounds having a composition range of $C_2AF$ to $C_6AF$. The $C_4AF$ phase is the average composition and constitutes about 8 – 13 % of a typical PC clinker. It results from the use of iron and aluminium raw materials to reduce the clinkerization temperature. It is basically

the phase that gives the gray color of cement. It hydrates very slowly and has little contribution to the strength.

### 2.2.3 Hydration of the OPC

In the presence of water, the abovementioned minerals separately combined with water to form the hydration products which contribute to set and strength development of the cement paste. The relative reaction rates and contributions to the early and late strength of each mineral in PC are summarized in Table 2.4.

**Table 2.4:** Relative properties of the main compounds of the OPC [38]

| | **$C_3S$** | **$C_2S$** | **$C_3A$** | **$C_4AF$** |
|---|---|---|---|---|
| **Reaction Rate** | Medium | Slow | Rapid | Medium |
| **Contribution to Strength:** | | | | |
| ***Early Strength*** | High | Low | Low | Low |
| ***Late Strength*** | High | High | Low | Low |

As can be seen from the Table 2.4, $C_3S$ and $C_2S$ are the main compounds responsible for the strength development of the cement paste. The typical hydration reactions of each compound are presented in the following sections.

#### 2.2.3.1 Alite and Belite

Both of the calcium silicate compounds ($C_3S$ and $C_2S$) of the Portland cement react with water to form the same two hydration products of calcium silicate hydrate (denoted as C-S-H gel) and calcium hydroxide (CH). The hydration reactions of alite and belite can be represented by equation (2.2) and (2.3), respectively.

$$2\ C_3S + 6\ H \longrightarrow C_3S_2H_3 + 3\ CH \quad (2.2)$$

$$2\ C_2S + 4\ H \longrightarrow C_3S_2H_3 + CH \quad (2.3)$$

Portland cement provides its strength and water-resistance mostly from the C-S-H gel. The CH formed in accordance with equations (2.2) and (2.3) cause a strongly basic environment with a high pH value of around 12 in the cement paste (and hence mortar and concrete) which inhibits the corrosion of embedded steel in reinforced concrete [39]. However, some of the dissolved CH by water leaking into the concrete may react with the $CO_2$ close to surface of the concrete according to equation (2.4) and produces both $CaCO_3$ and water. The water evaporates from the

$$CH + CO_2 \longrightarrow CaCO_3 + H \quad (2.4)$$

voids and this loss will cause shrinkage of the cement paste. As a result of *carbonation shrinkage* in concrete, cracks may occur close to surface and reduce the service life of the reinforced concrete structures [38].

#### 2.2.3.2 Aluminate and Ferrite

Hydration of $C_3A$ shows significant differences both in the presence and absence of sulphate. In the absence of sulphate, it reacts with water very rapidly and produces

$$C_3A + 21\ H \longrightarrow C_4AH_{13} + C_2AH_8 \quad (2.5)$$

unstable calcium alumina hydrates as indicated in equation (2.5). This rapid hydration of $C_3A$ releases excessive heat and may cause a sudden hardening of the cement paste, which is termed as *flash set*. Therefore, gypsum ($C\overline{S}H_2$) is generally ground with PC clinker as a retarder of the highly reactive $C_3A$ phase. In the presence of gypsum, the hydration reactions shown in equation (2.6) and (2.7) results in the formation of both $C_4A\overline{S}H_{12}$ (calcium monosulfoaluminate or AFm)

$$C_3A + C\overline{S}H_2 + 10\,H \longrightarrow C_4A\overline{S}H_{12} \quad (2.6)$$

$$C_3A + 3\,C\overline{S}H_2 + 26\,H \longrightarrow C_6A\overline{S}_3H_{32} \quad (2.7)$$

and $C_6A\overline{S}_3H_{32}$ (ettringite or AFt). The product $C_4A\overline{S}H_{12}$ is a semi-stable compound and may react with sulfate solutions penetrated into even the hardened cement paste at later ages according to reaction in equation (2.8). As a result of this reaction, cracks occur on the cement paste due to uncontrollable expansions resulting from

$$C_4A\overline{S}H_{12} + 2\,C\overline{S}H_2 + 16\,H \longrightarrow C_6A\overline{S}_3H_{32} \quad (2.8)$$

the conversion of $C_4A\overline{S}H_{12}$ into $C_6A\overline{S}_3H_{32}$. This situation is termed as *sulfate attack* in concrete.

$C_4AF$ reacts with water to form calcium alumina ferrite hydrates (analogue to ettringite) according to similar reactions in equation (2.6) and (2.7). The presence of iron oxide in the structure of $C_4AF$ leads to slower reaction rates than that of $C_3A$.

## 2.3 Sulfoaluminate-Belite Cement

### 2.3.1 General

SAB cement is produced by calcining natural materials such as limestone, bauxite and clay together with gypsum at temperatures around 1250-1350 °C in conventional rotary kilns. A variety of industrial wastes such as FGD waste, blast furnace slag, FBC ashes can also be utilized as part of the raw meal in order to reduce the consumption of expensive natural raw materials mentioned above.

There is an increasing interest and investigations toward SAB cement due to the following potential advantages over OPC [13-27]:

- Lower amounts of lime requirements in the raw meal for the formation of the main components calcium sulfoaluminate and belite which can also be formed at lower clinkerization temperatures of around 1250 °C as opposed to around 1450 °C. Lower clinkerization temperatures lead to significant energy savings during manufacturing.
- Substantially lower $CO_2$ emissions due to lower limestone utilization in raw meal. Total lime requirement of SAB cement is about 50 wt % as opposed to 65 wt %.
- Reduction in $NO_x$ emissions owing to lower clinkerization temperatures.
- Less energy is required for grinding relatively soft and friable SAB clinkers.
- Reduce the dependence on natural resources since a variety of industrial by-products such as fly ash, blast furnace slag, flue gas desulphurization waste etc. can be utilized as raw materials in the production.
- High resistance to sulfate attack since their phases are fully sulfated.

Consequently, this binder can give a substantial contribution to the saving of natural resources, energy and environment.

### 2.3.2 Chemical and Mineralogical Composition

Raw meal for SAB cement differs from those for OPC cement in that they contain significant amount of sulphate. SAB cement contains the mineral compounds of both calcium sulfoaluminate ($C_4A_3\overline{S}$) and belite ($C_2S$) as its major constituents. In addition to these compounds, they may contain ferrite ($C_4AF$) and anhydrite ($C\overline{S}$). High-lime content phases like alite ($C_3S$) and aluminate ($C_3A$) present in OPC do not exist in SAB cement.

The four principle mineral components of the SAB cement with their common names, chemical formulae and abbreviated notations are summarized in Table 2.5.

**Table 2.5:** Major mineral phases of SAB cement

| | **Calcium Sulfoaluminate** | **Dicalcium Silicate** | **Calcium Sulfate** | **Tetracalcium Aluminoferrite** |
|---|---|---|---|---|
| **Common Name** | Yeelimite or Klein's compound | Belite | Anhydrite | Ferrite |
| **Formulas** | 4CaO.3Al2O3.SO3 | $2CaO.SiO_2$ | $CaO.SO_3$ | $4CaO.Al_2O_3.Fe_2O_3$ |
| **Abbreviation** | $C_4A_3\overline{S}$ | $C_2S$ | $C\overline{S}$ | $C_4AF$ |

The relative amounts of the phases in SAB clinkers may vary in a wide range according to the type of the SAB cement as can be seen form the Table 2.6.

**Table 2.6:** The range of the amount of major phases in SAB cement, wt% [40]

| **Mineral Phases** | **SAB** |
|---|---|
| $\mathbf{C_4A_3\overline{S}}$ | 10-55 |
| $\mathbf{C_2S}$ | 10-60 |
| $\mathbf{C\overline{S}}$ | 0-25 |
| $\mathbf{C_4AF}$ | 0-40 |

The compounds of SAB cement have the following specific properties [35-37]:

**Calcium Sulfoaluminate:** $C_4A_3\overline{S}$ can be formed temperatures around 1250 °C and stable up to temperatures of 1350 °C. However, to preserve and prevent the dissociation of this phase, sintering temperatures in the production of SAB clinkers should not exceed 1300 °C. It can be considered as a substitute compound of $C_3S$

present in OPC and similarly provides sufficient early strength and rapid setting of the cement paste [25, 40].

**Belite:** It is usually present as β-$C_2S$ (larnite), but some α polymorph may also be present in the cement. Belite contributes only little to the strength of the cement at early ages, but it is the main phase responsible for the ultimate strength and durability of the hydrated cements [14,29,40].

**Ferrite:** The ferrite phase present in SAB cement possesses a higher reactivity than that present in OPC due to its formation at a lower temperature. It contributes to both the short-term and ultimate strength of the cement paste in addition to major contributions provided by $C_4A_3\overline{S}$ and $C_2S$ [30,40].

**Anhydrite:** $C\overline{S}$ is a necessary compound for the activation of $C_4A_3\overline{S}$ phase. If it is not present in the composition of SAB clinker, then gypsum ($C\overline{S}H_2$) addition to the clinker is required [19]. Together with $C_4A_3\overline{S}$ it contributes to the early strength development. It is also useful for strength increase at later ages by converting the existing CH and $AH_3$ into ettringite ($C_6A\overline{S}_3H_{32}$).

In addition to these phases, some other minor phases including CA (calcium mono-aluminate), $C_{12}A_7$ (mayenite), $C_2AS$ (gehlenite) and $C_5S_2\overline{S}$ (ternesite) may also be present in the SAB clinkers depending on the proportioning of the raw materials or insufficient heat treatment. Although CA and $C_{12}A_7$ exhibit a fast hydration, $C_2AS$ and $C_5S_2\overline{S}$ have very poor hydraulic properties and almost have no contribution to mechanical properties [14,40]

### 2.3.3 Hydration of the SAB Cement

The relative reaction rates and contributions to the early and late strength of each mineral in SAB cement are summarized in Table 2.7.

**Table 2.7:** Relative properties of the main compounds of the SAB cement

| | $C_4A_3\overline{S}$ | $C_2S$ | $C\overline{S}$ | $C_4AF$ |
|---|---|---|---|---|
| **Reaction Rate** | Rapid | Slow | Rapid | Medium |
| **Contribution to Strength:** | | | | |
| ***Early Strength*** | High | Low | Medium | Medium |
| ***Late Strength*** | Low | High | Medium | Medium |

The typical hydration reactions of each compound of SAB cement are presented in the following sections.

#### 2.3.3.1 Yeelimite and Anhydrite

The hydration of $C_4A_3\overline{S}$ yields the rapid formation of ettringite ($C_6A\overline{S}_3H_{32}$). The formation of ettringite provides the strength development during the early stages of hydration. The product $C_6A\overline{S}_3H_{32}$ shows expansive or non-expansive properties depending on the presence of free CaO (lime) or CH (calcium hydroxide or hydrated lime) in the system since microstructure of the ettringite is strongly dependent on the presence of lime [14,18,19,22,23,29,41,42]. Ettringite can be formed according to following reactions:

In the presence of free C or CH, ettringite forms as colloidal crystals according to reaction in equation (2.9) [41]. Ettringite formed by this reaction has expansive

$$C_4A_3\overline{S} + 8\,C\overline{S} + 6\,CH + 90\,H \longrightarrow 3\,C_6A\overline{S}_3H_{32} \qquad (2.9)$$

properties and is utilized in special applications requiring shrinkage resistant or self stressing cements [14,18].

In the absence of free C or CH, ettringite in the form of long lath-like crystals together with aluminium hydroxide ($AH_3$) are obtained according to reaction in equation (2.10). Ettringite synthesized by this reaction has non-expansive properties

$$C_4A_3\overline{S} + 2\,C\overline{S} + 38\,H \longrightarrow C_6A\overline{S}_3H_{32} + 2\,AH_3 \qquad (2.10)$$

and has the significant feature of giving high early strength in cementitious systems [14, 18,19,29,41,42].

**2.3.3.2 Belite and Ferrite**

Belite is a slow hydrating phase and reacts with water to give the products of C-S-H gel and CH according to reaction in equation (2.11) similar to the case in hydration of belite present in Portland cement. Strength development depends mostly on C-S-H gels in later ages.

$$2\,C_2S + 4\,H \longrightarrow C_3S_2H_3 + CH \qquad (2.11)$$

In the presence of non-reacted $C\overline{S}$, CH produced from reaction (2.11) can also react with the $AH_3$ obtained from reaction (2.10) to form ettringite which also provides additional strength gaining at later ages [22,29,40].

$$CH + AH_3 + C\overline{S} \longrightarrow C_6A\overline{S}_3H_{32} \qquad (2.12)$$

$C_4AF$ has a mineralizing effect on the formation of other phases of the cements and it was found that $C_4AF$ formed at lower clinkering temperatures hydrates more rapidly than $C_4AF$ present in Portland cement [30]. Therefore, this compound contributes to both the early and late strength in the sulfoaluminate belite systems [25]. Although cements high in $C_3A$ are prone to sulfate attack, those with high $C_4AF$ are not, possibly due to the substitution of iron in the monosulfate [35].

In the absence of free CaO, the ettringite formed within the first hours and days of hydration appears in the form of a fine crystals about 1-2 μm long. They fill the empty space between the cement particles. To prevent expansion, the formation of ettringite must take place in the absence of free calcium hydroxide. Under these conditions $C_4A_3\overline{S}$ hydrates rapidly and give a stable product of ettringite before the full development of skeletal structure and hardening of the cement paste. [29,40,42].

## 2.4 Fluidized Bed Combustion Ashes

Fluidized bed combustors generate mainly two streams of CCBs as fly and bottom ash. Fly ashes are the fine particles carried away by the flue gas and collected in a bag filter or electrostatic precipitator whereas bottom ashes are coarse spent materials removed from the bottom of the furnace. Both ashes contain the same type of minerals but in different proportions. [6,7].

FBC ashes contain coal derived calcined clay and unreacted free C, $C\overline{S}$ due to the utilization of limestone or dolomite as sorbent. The presence of considerable amount of free CaO and sulfate results in exothermal and expansive behaviors which make these wastes more difficult for both disposal in landfill and re-use in Portland cement and concrete industry. Furthermore, according to the various Portland cement standards, sulfate content in OPC should be between 2.5 and 4 % $SO_3$. This limitation also prevents their usage potential in the production of OPC [9,11,14,43,44]. The low operating temperatures of FBC systems leads to ashes having poor pozzolanic activity due to the reduced glass content related to the combustion temperature. As a result of this reduced ash reactivity toward CaO, their usage in blended Portland cement or concrete industry are also hindered [11,12,14]. However, according to a recent study performed for the investigation of the possibility of using FBC fly ashes for partial replacement of OPC, up to 30 wt % fly ash/OPC blends were found to meet compressive strength, setting time and soundness requirements of ASTM C 595 standard without any pre-hydration

treatment despite the nonconformity of FBC ashes to the standards designed for PCC fly ashes [58].

Therefore, in the absence of specific standards for FBC fly ashes and the presence of unburnt carbon in these ashes, the use of FBC ashes part of raw meal of special cements can be a solution for the problems mentioned above. FBC ashes in combination with other components of the raw meal can be considered as highly promising raw materials in the production of SAB clinkers containing sulfate based mineral phases like $C_4A_3\overline{S}$ and $C\overline{S}$. High amount of CaO content of the ashes as well as $SiO_2$, $Al_2O_3$ and $Fe_2O_3$ are efficiently evaluated for the formation of other phases of the SAB clinkers [9,17]. Ashes generated from fluidized bed combustion of low calorific value, high ash and sulfur content Turkish lignites contains high CaO and $SO_3$ besides their acidic oxide contents due to continuous limestone injection for $SO_2$ capture during combustion.

## 2.5 Literature Review

There exist numerous investigations on laboratory scale production of SAB cement [9-30]. In the light of these studies, SAB cement can be classified into the three major categories according to the content and proportions of the phase compositions. The tentative naming and some basic properties are summarized below:

1) *Calcium sulfoaluminate-rich belite cement:* They are mostly composed of only two main phases of SAB cement, the major component being $C_4A_3\overline{S}$ around 55-75 wt % and $C_2S$. Therefore, gypsum or anhydrite addition to the clinker is generally required to activate the $C_4A_3\overline{S}$ during hydration. This type of cement has been commercially manufactured and used in China for the past 30 years with current production being around one million tons per year. In other countries studies on this type of cement have already been performed in laboratory and pilot-scale plants but commercialization started

only recently by Lafarge Cement UK. This type of cement is typically used for applications requiring rapid setting and high early strength [13,14,17,19,45,46].

2) *Expansive belite-rich calcium sulfoaluminate cement:* Besides the main components of the SAB cement, they contain free lime up to 10 % which promotes expansion. More than 10 % of free lime content leads to decreases in strength at later ages due to unwanted high expansions. Belite constitutes the highest portion in such cement. This type of cement can be used in restricted areas requiring shrinkage-resistant and self-stressing cements [14,22,29,47].
3) *Non-expansive belite-rich calcium sulfoaluminate cement:* Cement having higher belite and lower $C_4A_3\overline{S}$ content than those of commercially produced SAB cement in addition to other phases with very low or totally deficient of free lime content. Industrial by-products with high sulfate content can be utilized in high percentages in the production. This type of cement show high mechanical strength both at early and late ages comparable to OPC and have the potential to replace it [13,14,17,25,29].

There is no commercial production of belite-rich calcium sulfoaluminate type of cement.

In the following sections, significant findings together with experimental conditions are explained in detail for each type of SAB cement.

### 2.5.1 Calcium Sulfoaluminate-Rich Belite Cement

In the study of *Belz et al.* [11], five different raw meals containing CFBC fly ash in the range of 29 to 42.3 wt % together with pure materials like $CaCO_3$, $Al_2O_3$ and other materials such as bauxite and red mud were prepared. The raw meal compositions were arranged to combine all available sulphate and silica into $C_4A_3\overline{S}$

and $C_2S$, respectively. Samples were burnt in a laboratory electric oven at temperatures ranging from 1100 to 1250 °C for two hours. After examining the mineral phases of the obtained clinkers, optimum sintering temperature where the highest XRD intensity occurred for $C_4A_3\overline{S}$ phase was found to lie in the range 1200 and 1250 °C. The cements were prepared by grinding the clinkers obtained with 18 wt % gypsum addition due to the inadequate sulfate content of them. High compressive strength values at early ages were obtained with the paste based on the cement sample having potential concentration of $C_4A_3\overline{S}$ as 52.5 wt %.

### 2.5.2 Expansive Belite-Rich Calcium Sulfoaluminate Cement

*Sahu et al.* [22] synthesized sulfoaluminate belite cements by using PCC fly ash, limestone and gypsum as raw materials. Raw meals were sintered in an electrical furnace at 1200 °C for half an hour and clinkers obtained were air cooled and ground in a mill to produce cements without gypsum addition. Cements were found to have free lime content in the range of 0 – 23.8 wt %. Free lime content up to 10 wt % in the produced SAB cements showed no harmful effect on the strength of the prepared mortars. However, mortars prepared by cements containing more than 10 wt % free lime displayed strength decreases at the later periods due to undesired expansion.

*Arjunan et al.* [20] utilized the industrial by-products such as lime kiln bag house dust, low-calcium fly ash and scrubber sludge to produce sulfoaluminate belite cements. Raw meals were sintered both in nodulized and powdered forms. The cement with a calculated free CaO content of 7.71 wt % was selected as the most promising one since the formation of both $C_4A_3\overline{S}$ and $C_2S$ were identified in this cement sample. These two minerals were formed at around 1250 °C with nodulized raw meal and at relatively lower temperature of 1175 °C with powdered raw meal. Compressive strengths for 1, 7 and 28 day curing ages for cement pastes made form the cement obtained at 1175 °C for 60 min confirm the usefulness of the cement.

### 2.5.3 Non-expansive Belite-Rich Calcium Sulfoaluminate Cement

*Mehta* [30] produced SAB cements with no free CaO but containing large amounts of belite with lower amounts of other phases as $C_4A_3\overline{S}$, $C_4AF$ and $C\overline{S}$ by utilizing pure reagent grade chemicals as high-purity $CaCO_3$, silicic acid, hydrated alumina, iron oxide and gypsum. The clinkers obtained by heating the raw meals in an electrical muffle furnace at 1200 °C for about 1 hour. Clinkers were ground to about 400 $m^2$/kg Blaine surface area without gypsum addition. In the case of Portland cements there are occasionally false-set problems due to decompostion of gypsum, which is normally interground with clinker. The microstructure examination of the clinkers show that $C_4A_3\overline{S}$ appears as cubic crystals whereas belite appears as large rounded grains. The clinkers were very easy to grind due to low burning temperature. One of the cements produced with potential mineral composition of 45 % $C_2S$, 20 % $C_4A_3\overline{S}$, 20 % $C\overline{S}$ and 15 % $C_4AF$ showed the unique property of developing early (1, 3, 7 days) strengths at rates similar to ordinary Portland cement and remarkably high strengths at later ages (28 and 120 days).

*Kasselouri et al.* [29] synthesized the non-expansive SAB cement having similar characteristics with OPC. Free CaO deficient clinker was obtained by sintering a mixture of limestone, gypsum, bauxite, silica sand and an iron-rich industrial by-product at 1280 °C. Cement was prepared by grinding the clinker without any supplementary addition of gypsum. The potential mineral composition of the cement was 47.1 % $C_2S$, 20.1 % $C_4A_3\overline{S}$, 19.8 % $C\overline{S}$ and 13.8 % $C_4AF$ and expansion tests of the prepared cement pastes confirm the specifications in the EN and ASTM standards for OPC.

Katsioti *et al.* [28] investigated the possibility of using the jarosite-alunite precipate, a waste product of a new hydrometallurgical process developed to treat economically low-grade nickel oxides ores, as a raw material for the production of SAB clinker. The raw meals were sintered at 1300 °C for 30 min and clinkers removed from the furnace left to cool inside a desiccator to avoid the effects of air

and moisture. The potential mineral composition of the cement was 46.25 % $C_2S$, 21.35 % $C_4A_3\overline{S}$, 19.80 % $C\overline{S}$ and 12.46 % $C_4AF$. The results of the physico-mechanical tests like grindability, setting times, compressive strengths and expansibility showed that the addition of jarosite–alunite precipitate did not negatively affect the quality of the produced SAB cement.

*Adolfsson et al.* [25] investigated the utilization potential of the slags originating from the steelmaking industry in the production of belite-rich cement activated with sulfoaluminate cement. Four raw meals including mixtures of the different type of the slags together with limestone, gypsum and an alumina rich material were prepared as briquettes and sintered at 1200 °C for 30 min. All mixtures were prepared to have a predominant phase, belite and with no free CaO content in cement according to the calculated potential phase compositions. X-ray diffraction and scanning electron microscopy results of the produced cements reveal that the formation of clinker phases of sulfoaluminate cements such as $C_2S$ and $C_4A_3\overline{S}$ was realized for all prepared mixtures and even when raw meal contained only ladle slag.

Studies on the production of SAB cements carried out to date at laboratory scale with their types, raw materials and experimental conditions are summarized in Table 2.8. As can be seen from the table, there exists no investigation on the production of non-expansive belite-rich sulfoaluminate cement from FBC ashes as raw material to date.

**Table 2.8:** Summary of the literature on the production of laboratory scale SAB cement

| Author | Year | Type of SAB Cement | Raw Materials | Synthesis Temp. and Holding Time | Cooling | Additional Gypsum to SAB Clinker |
|---|---|---|---|---|---|---|
| *Mehta* [30] | 1980 | 3 | High purity $CaCO_3$, silicic acid, hydrated alumina, iron oxide and gypsum | 1200 °C and 60 min | Not specified | No gypsum addition |
| *Thoreanu et al.* [47] | 1983 | 2 | Limestone, bauxite, phosphogypsum and belitic waste | 1300-1350 °C and 20 min | Not specified | No gypsum addition |
| *Sahu et al.* [22] | 1994 | 2 and 3 | Limestone, fly ash, gypsum | 1200 °C and 30 min | Air cooled | No gypsum addition |
| *Kasselouri et al.* [29] | 1995 | 3 | Limestone, gypsum, bauxite, silica sand, an iron-rich industrial by-product | 1280 °C and not specified | Not specified | No gypsum addition |
| *Arjunan et al.* [20] | 1999 | 2 and 3 | Bag house dust, class F fly ash and scrubber sludge | 1175,1250 °C and 30, 45 and 60 min | Natural Air Cooled | No gypsum addition |
| *Kalogridis et al.* [42] | 2000 | 3 | Limestone, bauxite, siliceous earth, an iron-rich industrial by-product, gypsum | 1280 °C and not specified | Not specified | No gypsum addition |

**Table 2.8:** Summary of the literature on the production of laboratory scale SAB cement (Cont'd)

| Author | Year | Type of SAB Cement | Raw Materials | Synthesis Temp. and Holding Time | Cooling | Additional Gypsum to SAB Clinker |
|---|---|---|---|---|---|---|
| *Belz et al.* [11] | 2005 | 1 | FBC fly ash, bauxite, red mud, pure $CaCO_3$ and $Al_2O_3$ | 1100-1250 °C and 120 min | Not specified | 18 wt % of the cement |
| *Katsioti et al.* [28] | 2006 | 3 | Limestone, schist, bauxite, gypsum and jarosite-alunite precipitate | 1300 °C and 30 min | Inside a desiccator | No gypsum addition |
| *Belz et al.* [12] | 2006 | 1 | Limestone, fly ash, FGD waste, bauxite, FBC fly ash and FBC bottom ash | 1200 -1300 °C and 120 min | Not specified | Not specified |
| *Adolfsson et al.* [25] | 2007 | 3 | Limestone, alumina-rich material, gypsum and steelmaking slags | 1200 °C and 30 min | Water cooling | No gypsum addition |
| *Jewell et al.* [48] | 2007 | 1 | Limestone, bauxite, PCC fly ash, CFBC bottom ash | 1250 °C and 60 min | Air cooled | 15-20 wt % of the cement |

**1:** *Calcium sulfoaluminate-rich belite cement*
**2:** *Expansive belite-rich calcium sulfoaluminate cement*
**3:** *Non-expansive belite-rich calcium sulfoaluminate cement*

# CHAPTER 3

# EXPERIMENTAL STUDY

## 3.1 General

In the extent of this study, chemical and physical properties of the ashes generated from fluidized bed combustion (FBC) of a typical Turkish lignite, limestone, bauxite and gypsum were initially determined. Afterwards, the raw meal of the non-expansive belite-rich sulfoaluminate cement was prepared from the abovementioned raw materials according to modified Bogue calculations. Raw meal was subjected to initially thermal analysis and then sintered in a muffle furnace. Finally, chemical, mineralogical and morphological properties of the obtained clinkers and cements were examined.

## 3.2 Raw Materials

The FBC ashes previously generated by firing a typical Turkish lignite with limestone addition in a 0.3 $MW_t$ Atmospheric Bubbling Fluidized Bed Combustion (ABFBC) Test Rig were used as solid waste constituent of the raw meal [49].

The lignite and limestone utilized in the firing tests were supplied by Çan 2 x 160 MW Circulating Fluidized Bed (CFB) Thermal Power Plant and Çayırhan Thermal Power Plant of Park Thermic, Electric Industry and Trade, Inc., respectively. The lignite originates from Çan reserves of Turkish Coal Enterprises. Limestone was provided from Acıbaşı limestone quarry, 10 km away from the Çayırhan Thermal Power Plant. Analysis of Çan lignite is given in Table 3.1. As can be seen from the

table, it is a high sulfur and high ash content lignite and therefore was burnt in its own ash with limestone addition.

**Table 3.1:** Analysis of Çan lignite [49]

| **Proximate Analysis (As received basis)** | | **Ultimate Analysis (Dry Basis)** | |
|---|---|---|---|
| **Moisture, %** | 16.48 | **C, %** | 44.93 |
| **Volatile Matter, %** | 31.05 | **H, %** | 4.09 |
| **Fixed Carbon, %** | 25.74 | **N, %** | 1.14 |
| **Ash, %** | 26.74 | **O, %** | 13.96 |
| | | **S, %** | 3.86 |
| **LHV, MJ/kg** | 13.30 | **Ash, %** | 32.02 |

Ash analysis of the lignite given in Table 3.2 shows that acidic oxide content is significantly higher than basic oxide content which is typical of Turkish lignites.

**Table 3.2:** Ash analysis of Çan lignite, wt % [49]

| **Components** | **Ash** |
|---|---|
| **$SiO_2$** | 56.56 |
| **$Al_2O_3$** | 17.49 |
| **$Fe_2O_3$** | 10.99 |
| **CaO** | 9.21 |
| **MgO** | 0.57 |
| **$SO_3$** | 2.05 |
| **$Na_2O$** | 1.45 |
| **$K_2O$** | 0.31 |
| **$TiO_2$** | 1.38 |
| **Total** | 100.00 |

However, acidic oxide content of the generated ash gets lower when burnt with limestone addition in FBC systems. The lignite fed to the combustor was below 16 mm in size and had $d_{50}$ of 3.56 mm. Limestone on the other hand, had particle size below 1.18 mm with a $d_{50}$ of 0.41 mm. Operating conditions of the firing test from which ashes were generated are shown in Table 3.3. Details of the continuously operated test rig can be found elsewhere [49].

**Table 3.3:** Operating conditions of the firing test [49]

| **Parameter** | **Firing Test** |
|---|---|
| Coal flow rate, kg/h | 69 |
| Limestone flow rate, kg/h | 22 |
| Ca/S molar ratio (added) | 3 |
| Bed drain flow rate, kg/h | 8 |
| Cyclone ash flow rate, kg/h | 19 |
| Baghouse ash flow rate, kg/h | 1.2 |
| Air flow rate, kmol/h | 14 |
| Excess air, % | 21 |
| Superficial velocity, m/s | 1.9 |
| Average bed temperature, °C | 848 |
| Average freeboard temperature, °C | 817 |
| Bed height, m | 1.1 |
| Bed pressure drop, cm $H_2O$ | 63 |

In addition to FBC ashes, the limestone used for desulfurization in the test rig, bauxite and gypsum were utilized as the usual remaining components of the sulfoaluminate based cement raw meal. Chemical composition of all raw materials with loss on ignition (LOI) values are presented in Table 3.4

**Table 3.4:** Chemical analysis of raw materials, wt %

| Components | Limestone | Bottom Ash | Baghouse Filter Ash | Bauxite | Gypsum |
|---|---|---|---|---|---|
| **LOI** | 43.343 | 2.086 | 4.095 | 14.551 | 0.000 |
| **CaO** | 50.291 | 17.545 | 14.665 | 0.070 | 45.558 |
| **$SiO_2$** | 1.957 | 50.529 | 46.399 | 0.000 | 0.000 |
| **$Al_2O_3$** | 0.381 | 13.777 | 6.530 | 68.261 | 0.294 |
| **$Fe_2O_3$** | 0.540 | 3.754 | 9.358 | 16.954 | 0.285 |
| **$SO_3$** | 0.000 | 7.281 | 14.775 | 0.000 | 53.554 |
| **MgO** | 3.157 | 1.093 | 1.217 | 0.076 | 0.281 |
| **$K_2O$** | 0.181 | 1.641 | 0.856 | 0.039 | 0.014 |
| **$Na_2O$** | 0.150 | 2.294 | 2.106 | 0.049 | 0.016 |
| **Total** | 100.000 | 100.000 | 100.000 | 100.000 | 100.000 |

As received photographs of all raw materials are demonstrated in Figure 3.1.


**Figure 3.1:** As received photographs of all raw materials

## 3.3 Raw Meal Preparation

The particle size of the raw meal should be fine enough to achieve higher area of contact and conversion as the main reactions occur in solid state [8,50,51]. Therefore, all raw materials except baghouse filter ash were subjected to size reduction. Bauxite rocks and bottom ash were first crushed by using roller crusher. All the raw materials were dried in an oven at 105 °C for 24 h and ground to pass 140 mesh sieve (106 μm) before mixing [42,50,52,53].

Raw meal was then prepared by mixing raw materials in such proportions to get the chemical and mineralogical composition of the desired belite-rich sulfoaluminate cement according to modified Bogue calculations, detailed in Appendix A. The raw meal preparation calculations are based on chemical analysis of raw materials from which mass balances can be performed [25,44]. As a result of these computations the raw meal was prepared by blending the raw materials in the weight proportions presented in Table 3.5.

**Table 3.5:** Composition of the raw meal, wt %

| | **Limestone** | **Bottom Ash** | **Baghouse Filter Ash** | **Bauxite** | **Gypsum** |
|---|---|---|---|---|---|
| **Raw Meal** | 50 | 10 | 15 | 10 | 15 |

Theoretical chemical analysis of the raw meal calculated by using the weight proportions given in Table 3.5 and chemical analysis of each raw material together with chemical composition of clinker by eliminating the LOI value of the raw meal are shown in Table 3.6.

**Table 3.6:** Theoretical chemical analysis of the raw meal and clinker, wt %

| Components | Raw Meal (Theoretical) | Clinker (Theoretical) |
|---|---|---|
| **LOI** | 23.509 | 0.000 |
| **CaO** | 35.979 | 47.036 |
| **$SiO_2$** | 13.473 | 17.613 |
| **$Al_2O_3$** | 8.937 | 11.684 |
| **$Fe_2O_3$** | 3.715 | 4.857 |
| **$SO_3$** | 11.432 | 14.945 |
| **MgO** | 1.908 | 2.494 |
| **$K_2O$** | 0.399 | 0.522 |
| **$Na_2O$** | 0.649 | 0.848 |
| **Total** | 100.000 | 100.000 |

Potential Bogue mineralogical composition of the clinker based on the theoretical chemical composition of the SAB clinker in Table 3.6 is given in Table 3.7.

**Table 3.7:** Theoretical Bogue mineral composition of the SAB clinker, wt%

| Mineral Phases | Clinker |
|---|---|
| **$C_2S$** | 48.717 |
| **$C_4A_3\overline{S}$** | 16.286 |
| **$C_4AF$** | 14.244 |
| **$C\overline{S}$** | 20.753 |

The blended raw meal was homogenized in a ceramic ball mill (Figure 3.2) for 60 min [54,55]. Raw meal was also subjected to chemical analysis after homogenization operation.

**Figure 3.2:** Ceramic ball mill

Homogenized raw meal and all raw materials ground to pass 140 mesh sieve were subjected to particle size distribution (PSD) analysis. Malvern Mastersizer 2000 particle sizing system by a laser scattering analyzer with assured measurement performance from 0.02 micron to 2 millimeter is utilized for PSD analysis. The analyzer allows a rapid interchange between wet and dry measurements which require about 200 mg and 10 g of sample, respectively. PSD measurements of all materials except gypsum were performed by wet method. Wet dispersion was achieved using the Hydro 2000 Micro Precision dispersion unit with distilled water and dry dispersion was carried out using the Scirocco 2000 dry powder feeder with a micro volume powder feeder tray under air vacuum. The obstruction value was monitored during analysis and it was kept in ideal ranges, i.e., between 5% and 20% for wet measurements and 0.5% to 5% for dry measurements [56, 57].

It was preferred to use dry measurement for gypsum due to steady decrease of obstruction value with gypsum during wet measurement. The decrease in obstruction value generally aroused from the dissolution of the inspected sample in water. Although pure gypsum is nearly insoluble in water, some impurities present in gypsum may dissolve and leads to decrease in obstruction value during wet measurement.

## 3.4 Thermal Analysis

Thermal analysis of the raw meal was carried out in Setaram Labsys TGA/DTA which is thermal analysis equipment that performs both TGA and DTA simultaneously on the same sample. It determines the weight change of the sample and measures the change in temperature between the sample and the reference while they are subjected to a controlled temperature program. 13 mg of the raw meal was placed in a alumina crucible and subjected to a programmed heating of 10 °C/min in an air atmosphere, up to 1300 °C, where it was kept for 20 min [25,59,60].

The results of thermal analyses were corrected by extracting the values obtained with a run of empty crucibles at the same conditions from the experimental results to eliminate the possible effects originated from equipment [25].

## 3.5 Furnace Sintering

The raw meal was placed in platinum crucibles, as shown in Figure 3.3, and was sintered in a laboratory scale muffle furnace with an air atmosphere for different residence times at maximum temperatures ranging from 1200 °C to 1300 °C. It was followed by cooling moderately fast rates in direct natural air to reduce the glass formation and preserve the desired crystalline minerals of the clinkers [20,22,34,37,53].

**Figure 3.3:** Raw meal in platinum crucible

Heating profiles for each set with heating rates and holding times are shown in Appendix B. As can be seen from heating profiles for each set, raw meal was heated to the maximum temperatures with a pause of 30 min at around 800 °C to allow for the escape of $CO_2$ from carbonates [20,61]. The clinkers formed were ground to powder form to produce cements without any supplemantary addition [29,30,42].

## 3.6 X- ray Powder Diffraction (XRD)

A Rigaku DMAX 2200, vertical multi-purpose X-ray diffractometer with CuKα radiation (λ = 1.54056 Ä, 40kV and 40mA) diffracted beam monochromator and high linearity scintillation counter equipment was utilized for qualitative identification of unknown crystalline phases of the cement samples. The analyzed materials were finely ground to powder and homogenized. The powder patterns were gathered over the 2Θ range of 1-60° [20,28,29,43].

## 3.7 Scanning Electron Microscopy (SEM)

The Jeol JSM-6400 electron microscope configured with a Noran energy dispersive spectrometer (EDS) was utilized to investigate morphology and elemental composition information of clinker phases in direct relation to the SEM images. It can examine and analyze samples at magnifications from 5X to 200,000X. Fractured clinker sample was coated by a thin layer of gold to prevent surface charge accumulation and to promote electrical conductivity [20].

# CHAPTER 4

# RESULTS AND DISCUSSION

## 4.1 General

In this thesis study, the effect of using FBC ashes as a constituent of raw meal on the production of laboratory scale non-expansive belite-rich sulfoaluminate cement was investigated. This was achieved by examining the items listed below:

- Particle size distribution of all raw materials and raw meal
- Thermal analysis of raw meal
- Chemical analysis of the raw meal and cements
- Mineralogical and morphological analyses of cement and clinker samples, respectively

## 4.2 Particle Size Distributions

Particle size distributions of both the ground raw materials and the raw meal are shown in Figure 4.1. As can be seen from the figure, the particle sizes of bauxite and bottom ash are larger than those of other constituents due to their higher grindability work indices and due to the fact that each constituent of the raw meal was subjected to the same grinding operation. It can also be noted that the PSD of the raw meal lies within the range of PSDs of limestone, baghouse filter ash and gypsum as those components form almost 80 wt % of the mixture.

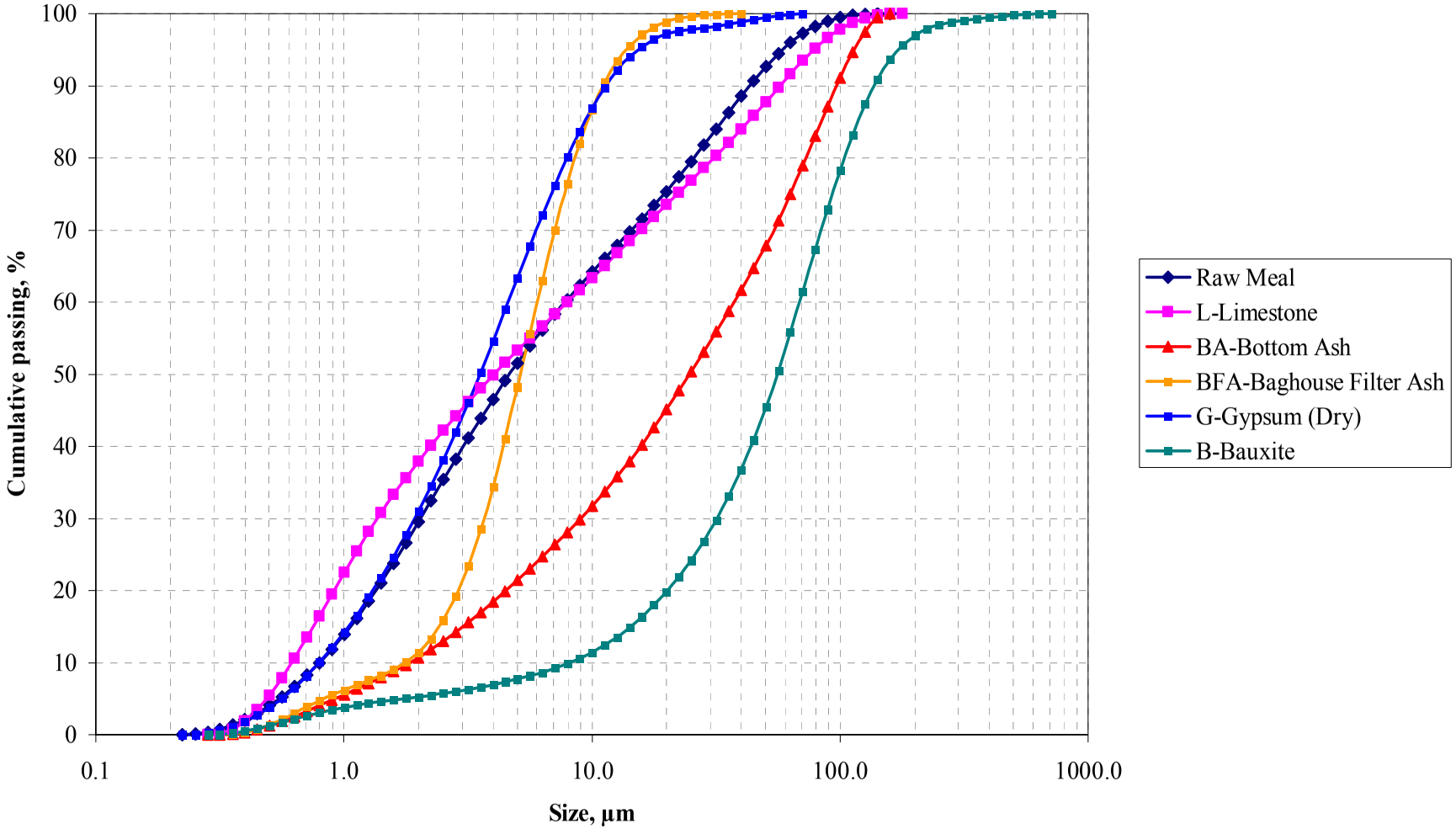


**Figure 4.1:** Particle size distributions of raw materials and raw meal

Table 4.1 summarizes $d_{10}$, $d_{50}$ and $d_{90}$ of particle size distributions of each constituent and the raw meal. As can be seen from the table, $d_{50}$ of the raw meal is around 5 μm which is even finer than those utilized in the study of *Adolfsson et al.* [25] where $d_{50}$ of 15-20 μm was found not to cause any critical problem on the properties of the cement produced. Therefore particle size of raw meal can be considered to be fine enough to get an improved burnability and reactivity.

**Table 4.1:** $d_{10}$, $d_{50}$ and $d_{90}$ of values for each raw material and raw meal

| | **Diameter on cumulative, μm** | | |
|---|---|---|---|
| **Materials** | **$d_{10}$** | **$d_{50}$** | **$d_{90}$** |
| Limestone | 0.617 | 4.030 | 57.407 |
| Bottom ash | 1.852 | 24.770 | 97.127 |
| Bag house filter | 1.779 | 5.176 | 11.091 |
| Bauxite | 8.172 | 55.829 | 137.674 |
| Gypsum | 0.796 | 3.534 | 11.386 |
| **RM** | **0.799** | **4.677** | **43.121** |

Particle size distributions in tabulated forms and their corresponding frequency curves can be found in Appendix C and Appendix D, respectively.

## 4.3 Thermal Analysis

Homogenized raw meal was subjected to thermal analysis to examine the effect of the addition of FBC ashes to raw meal on the weight losses, temperatures and sequence of the reactions taking place during the heating operation.

Thermogravimetry (TG) and differential thermogravimetry (DTG) curves are presented in Figure 4.2. As can be seen from the figure, there exists four distinct weight loss peaks in DTG curve at temperatures of 123, 515, 793 and 1280 °C.

Examination of the information provided by TG analysis including temperature ranges of the significant weight losses, corresponding percentages and basic considerations on the source of these losses are summarized in Table 4.2. The first loss at 100-140 °C, with about 1.5 wt %, refers to partial or complete dehydration of gypsum. The peak at 500 - 550 °C is considered to be due to dehydration and decomposition of bauxite. Some of $MgCO_3$ present in raw meal may also be decarbonated at this temperature range. The most significant weight loss, with about

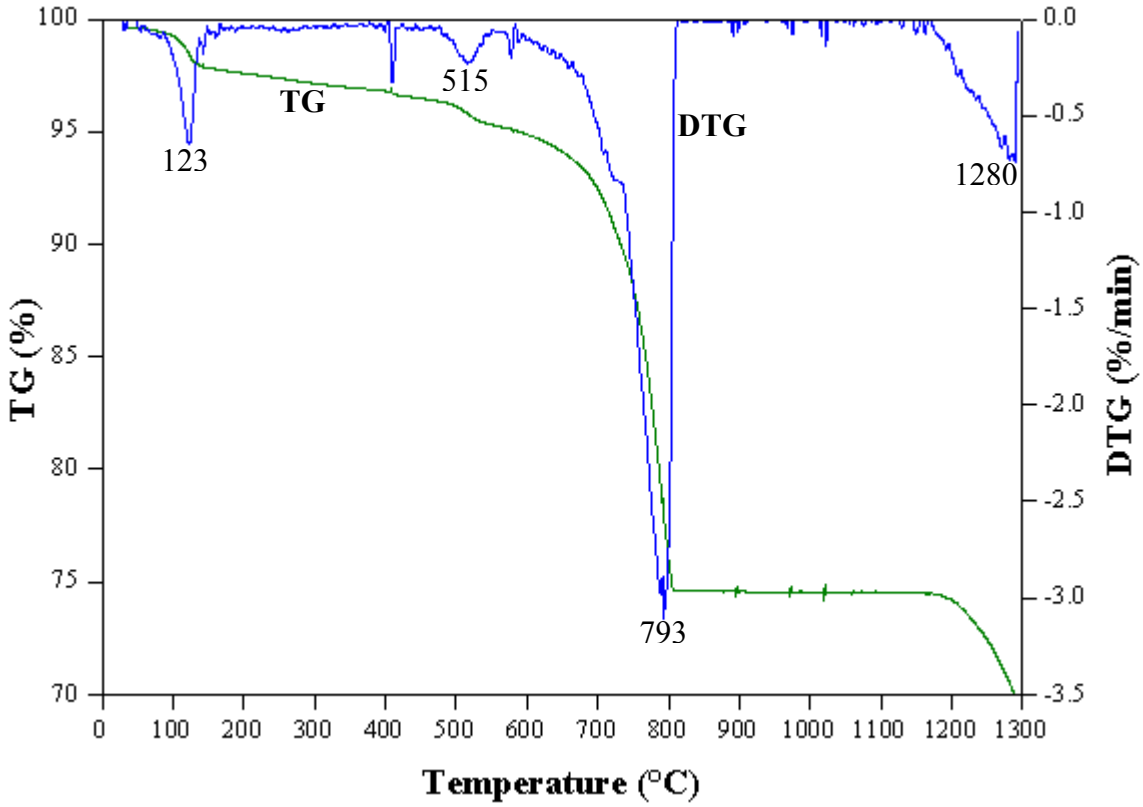


**Figure 4.2:** TG / DTG curves of the raw meal

18 wt %, occurs in the temperature range of 700 - 810 °C due to the release of $CO_2$ during decomposition of the $CaCO_3$ which is the major component present in limestone. The final loss at 1190 – 1290 °C, with about 5 wt %, may be due to some dissociation of $CaSO_4$ into CaO and $SO_3$ [15,25,34,35].

**Table 4.2:** Summary of the TG results of the raw meal

| Temperature Range (°C) | Weight Loss (%) | Remark |
|---|---|---|
| 100 - 140 | 1.35 | Dehydration of Gypsum |
| 500 - 550 | 0.81 | Decomposition of Bauxite |
| 700 - 810 | 17.78 | Dissociation of $CaCO_3$ |
| 1190 - 1290 | 4.75 | Dissociation of $CaSO_4$ |
| **30 – 1290** | **30.39** | **Total weight loss** |

Differential thermal analysis (DTA) curve together TG curve is shown in Figure 4.3. As can be seen from the figure, the minima and maxima peaks occur on DTA curve

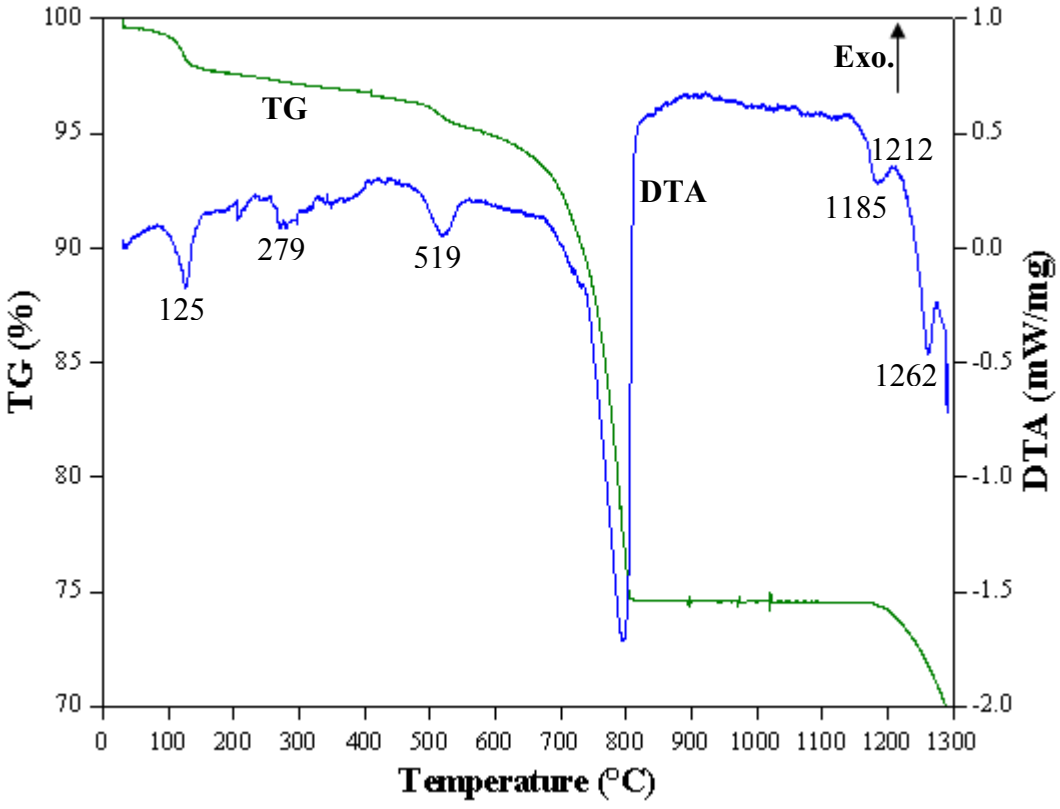


**Figure 4.3:** TG / DTA curves of the raw meal

due to reactions taking place during heating. The temperature of the sample will either decrease or increase relative to that of reference empty inert crucible as the reaction absorbs heat (endothermic reactions, minima on DTA curve) or releases heat (exothermic reactions, maxima on DTA curve), respectively. Therefore, RM exhibits endothermic effects at temperatures of around 125, 279, 519 and 794 °C followed by both endothermic and exothermic effects at higher temperatures. The endothermic effects observed up to 794 °C belong to dehydration or decomposition reactions of gypsum, bauxite, $MgCO_3$, calcite and other possible minerals present in FBC ashes like illite, hematite and feldspar [58]. At higher temperatures, formation and decomposition reactions of the minor minerals like $C_2AS$ (gehlenite), CA (calcium mono-aluminate), $C_{12}A_7$ (mayenite) and $C_5S_2\overline{S}$ (ternesite) occur to produce desired minerals of the calcium sulfoaluminate clinker, i.e; $C_4A_3\overline{S}$ (yeelimite), $C_2S$ (belite), $C_4AF$ (ferrite) and $C\overline{S}$ (anhydrite). The formation of calcium sulfoaluminate, $C_4A_3\overline{S}$, can take place through a homogeneous solid state reaction according to equation (4.1) and through a heterogeneous solid-gas reaction with sulfur dioxide and oxygen according to equation (4.2) since decomposition of $C\overline{S}$ (anhydrite), starts at lower temperatures like 1000 °C in the presence of coal ash [40].

$$3C_{12}A_7 + 7C\overline{S} \longrightarrow 7C_4A_3\overline{S} + 15C \qquad (4.1)$$

$$3C_3A + SO_2 + 1/2O_2 \longrightarrow C_4A_3\overline{S} + 6C \qquad (4.2)$$

The position and intensity of the peaks between 1000 and 1300 °C are good indicators of the burnability of the raw meal. Therefore, additions of FBC ashes around 25 wt % to the raw meal do not seem to affect typical clinkerization reactions and temperatures.

## 4.4 Furnace Trials

Chemical analysis of the homogenized raw meal is given in Table 4.3 together with the theoretical analysis calculated by using the weight proportions and chemical composition of each raw material given in Table 3.6 for comparison purposes. Inspection of the two analysis show that there is no significant difference in the chemical composition of raw meal originating from homogenization operation.

**Table 4.3:** Chemical composition of the raw meal, wt%

| Components | Raw Meal (Theoretical) | Raw Meal (Experimental) |
|---|---|---|
| **LOI** | 23.509 | 23.940 |
| **CaO** | 35.979 | 36.398 |
| **$SiO_2$** | 13.473 | 12.900 |
| **$Al_2O_3$** | 8.937 | 9.208 |
| **$Fe_2O_3$** | 3.715 | 4.074 |
| **$SO_3$** | 11.432 | 10.768 |
| **MgO** | 1.908 | 1.489 |
| **$K_2O$** | 0.399 | 0.322 |
| **$Na_2O$** | 0.649 | 0.900 |
| **Total** | 100.000 | 100.000 |

This raw meal was subjected to furnace sintering at temperatures of 1200, 1250 and 1300 °C for various holding times. The selected maximum temperatures are in agreement with the results of thermal analysis of the raw meal and are also confirmed by previous findings on the production of sulfoaluminate-belite cement [20,28].

The first set of sintering experiments (SET 1) was carried out at the lowest temperature for holding times of 30, 45 and 60 min. The clinkers obtained are

denoted by CK1, CK2 and CK3 in the order of increasing holding time. As can be seen from the photographs of the clinkers (Figure 4.4), all have similar light brown


**Figure 4.4:** Photographs of clinkers CK1, CK2 and CK3

color and display shrinking behavior. Change of weight before and after ignition with corresponding percent weight losses for each sample are tabulated in Table 4.4. As can be seen from the table, weight loss of all samples is around 25 wt %.

**Table 4.4:** Sample weights before and after ignition for SET 1

| | **SET 1** | | |
|---|---|---|---|
| | **CK1** | **CK2** | **CK3** |
| **Before ignition, gr** | 20.380 | 20.510 | 20.420 |
| **After ignition, gr** | 15.330 | 15.410 | 15.320 |
| **Weight loss, %** | 24.779 | 24.866 | 24.976 |

The second and third sets of sintering experiments (SET 2 and SET3) were carried out at the temperatures of 1250 and 1300 °C for 60 min, respectively. The photographs of the obtained clinkers were shown in Figure 4.5. These clinkers have a darker color than those of CK1 to CK3 reflecting improved level of sintering due to exposing higher temperatures [48].

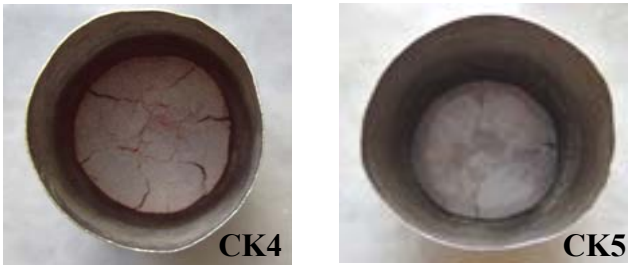


**Figure 4.5:** Photographs of clinkers CK1, CK2 and CK3

Change of weight before and after ignition with corresponding percent weight losses for each sample are presented in Table 4.5. The weight losses of the samples for SET 2 and 3 are around 1-2 percentage points higher than those of SET 1. These additional losses may have originated from $SO_2$ release due to dissociation of $CaSO_4$ at the higher temperatures of the SET 2 and 3.

**Table 4.5:** Sample weights before and after ignition during SET 2 and 3

| | **SET 2** | **SET 3** |
|---|---|---|
| | **CK4** | **CK5** |
| **Before ignition, gr** | 20.980 | 22.450 |
| **After ignition, gr** | 15.630 | 16.460 |
| **Weight loss, %** | 25.500 | 26.681 |

## 4.5 Chemical Analysis

Typical appearance of cements obtained by grinding the sintered clinkers is shown in Figure 4.6.

**Figure 4.6:** Photographs of the cement C4

The results of experimental chemical analysis and the corresponding modified Bogue potential mineralogical composition of the cements obtained for SET 1 are given in Table 4.6 and Table 4.7, respectively. Comparison between the experimental values contained in Table 4.6 and Table 4.7 and theoretical ones contained in Table 3.6 and Table 3.7 exhibits some differences particularly in mineralogical compositions due to the sensitivity of derived Bogue formulae to slight changes in chemical composition. For instance, the percentage of the $C_2S$ in the cement C2 is relatively higher compared to those in cements C1 and C3 due to higher silicon dioxide content in the representative sample of the cement C2.

**Table 4.6:** Chemical composition of cements C1, C2 and C3, wt %

| | **Cements** | | |
|---|---|---|---|
| **Components** | **C1** | **C2** | **C3** |
| **LOI** | 0.000 | 0.000 | 0.000 |
| **CaO** | 50.754 | 47.850 | 53.831 |
| **$SiO_2$** | 14.475 | 20.854 | 13.282 |
| **$Al_2O_3$** | 9.814 | 9.514 | 12.107 |
| **$Fe_2O_3$** | 7.323 | 5.964 | 5.456 |
| **$SO_3$** | 14.268 | 12.466 | 11.845 |
| **MgO** | 2.677 | 2.463 | 2.423 |
| **$K_2O$** | 0.367 | 0.511 | 0.394 |
| **$Na_2O$** | 0.323 | 0.381 | 0.661 |
| **Total** | 100.00 | 100.00 | 100.00 |

**Table 4.7:** Potential mineralogical composition of cements C1, C2 and C3, wt %

| | Cements | | |
|---|---|---|---|
| **Mineral Phases** | **C1** | **C2** | **C3** |
| **$C_2S$** | 41.543 | 55.501 | 38.119 |
| **$C_4A_3\overline{S}$** | 10.107 | 10.412 | 16.976 |
| **$C_4AF$** | 22.284 | 16.829 | 16.603 |
| **$C\overline{S}$** | 21.926 | 17.258 | 16.243 |

The results of experimentally determined chemical composition and the corresponding modified Bogue potential mineralogical composition of the cements obtained for SET 2 and 3 are given in Table 4.8 and Table 4.9, respectively.

**Table 4.8:** Chemical composition of cements C4 and C5, wt %

| | Cements | |
|---|---|---|
| **Components** | **C4** | **C5** |
| **LOI** | 0.000 | 0.000 |
| **CaO** | 44.480 | 41.205 |
| **$SiO_2$** | 15.361 | 17.445 |
| **$Al_2O_3$** | 19.568 | 21.759 |
| **$Fe_2O_3$** | 5.384 | 5.250 |
| **$SO_3$** | 11.732 | 10.704 |
| **MgO** | 2.547 | 2.412 |
| **$K_2O$** | 0.445 | 0.358 |
| **$Na_2O$** | 0.484 | 0.868 |
| **Total** | 100.000 | 100.000 |

**Table 4.9:** Potential mineralogical composition of cements C4 and C5, wt %

| | Cements | |
|---|---|---|
| **Mineral Phases** | **C4** | **C5** |
| **$C_2S$** | 42.023 | 44.625 |
| **$C_4A_3\overline{S}$** | 30.279 | 32.310 |
| **$C_4AF$** | 15.617 | 14.239 |
| **$C\overline{S}$** | 12.080 | 8.826 |

The high percentage of the $C_4A_3\overline{S}$ with respect to theoretical value presented in Table 3.7 is considered to be due to higher alumina oxide value measured in these samples. The amounts of $C_2S$ phase for both of these cements were found close to that of theoretical value.

## 4.6 X-ray Powder Diffraction (XRD)

The powder XRD patterns of the cements C1, C2 and C3 are given in Figure 4.7. The assignment of the peaks were accomplished by comparing both the values of 2Θ and relative intensity with peak points of the cements and those of possible minerals of the SAB cement. 2Θ values and relative intensities of the peak points with those of possible minerals for each cement are given in Appendix E in tabulated form.

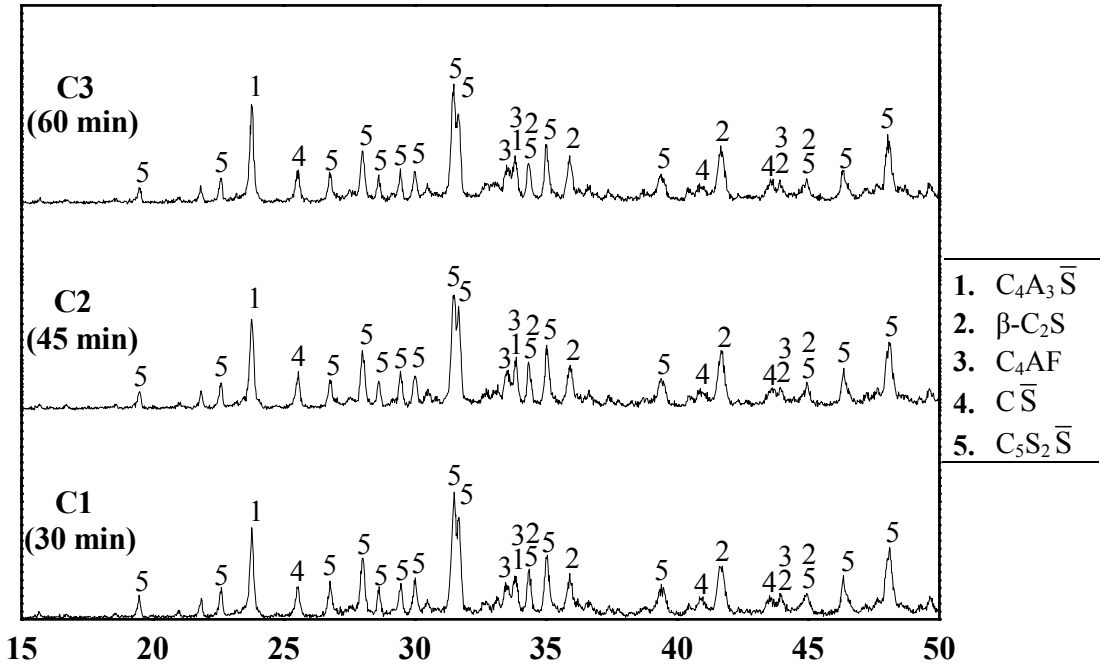


**Figure 4.7:** XRD powder patterns for cements C1, C2, and C3

The Joint Committee on Powder Diffraction Standards (JCPDS) line patterns of $C_4A_3\overline{S}$, β-$C_2S$, $C_4AF$, $C\overline{S}$ and $C_5S_2\overline{S}$ minerals with XRD patterns of the obtained cements for SET 1 are also given in Figure 4.8.

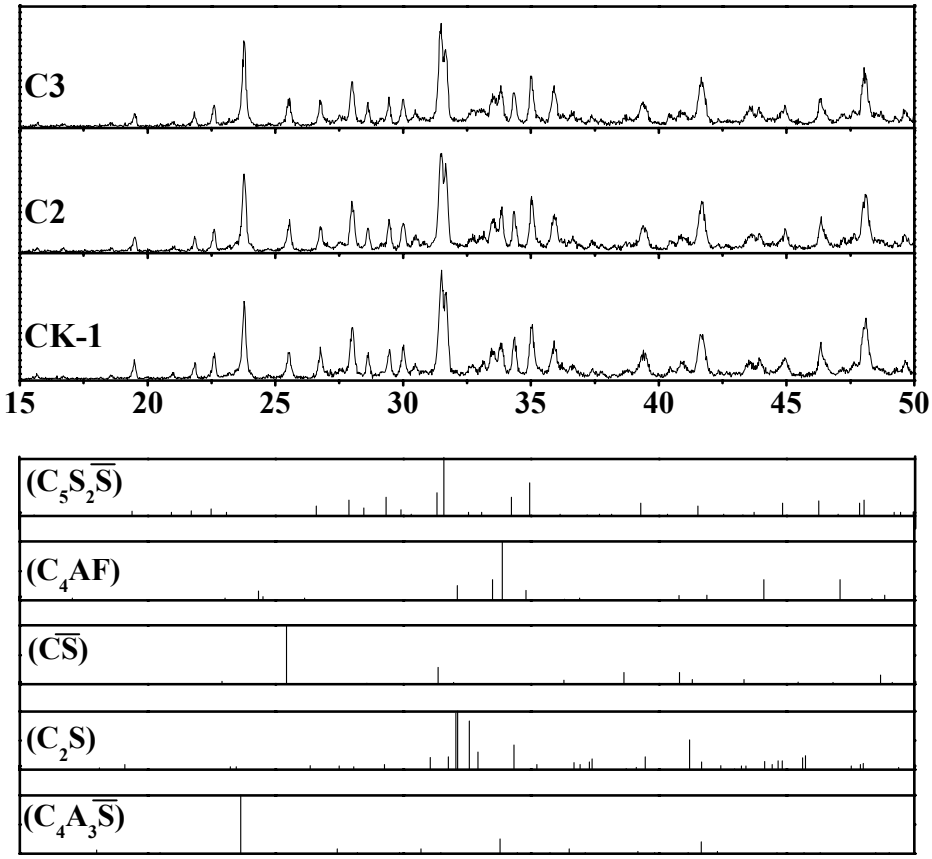


**Figure 4.8:** Comparison of XRD pattern of cements C1, C2 and C3 with standard line patterns of expected minerals

As can be seen from these figures, similar peaks were obtained for all of the three cements with formation of yeelimite (1), larnite (2), brownmillerite (3), anhydrite (4) as hydraulically active desired minerals and formation of ternesite (5) as hydraulically poor undesired phase [11,12,48]. It is worth noting that another hydraulically inactive undesired mineral, $C_2AS$ (gehlenite), is absent. This is indicative of the fact that final sintering temperature of 1200 °C was sufficiently

high for dissociation of this mineral to form $C_4A_3\overline{S}$ and $C_5S_2\overline{S}$. Ternesite remains in all cements obtained for SET 1 independent of the residence time. The presence of this mineral is likely to be due to either lower sintering temperature or residence time than required to decompose it to β-$C_2S$ and $C\overline{S}$ [40,43]. Some of the peaks belonging to β-$C_2S$ mineral are not clearly detected by XRD due to presence of the silicate in the form of $C_5S_2\overline{S}$. Comparison between the intensity of the peaks belonging to hydraulically active minerals ($C_4A_3\overline{S}$, β-$C_2S$, $C_4AF$ and $C\overline{S}$) for residence times of 30, 45 and 60 min (Appendix E) reveals that the intensity increases with residence time. Therefore, residence time of 60 min was chosen for SET 2 and SET 3 conducted at higher final sintering temperatures.

Figure 4.9 shows the powder XRD patterns of the cements C4 and C5 produced at final sintering temperature of 1250 °C and 1300 °C with residence time of 60 min for SET 2 and SET 3, respectively.

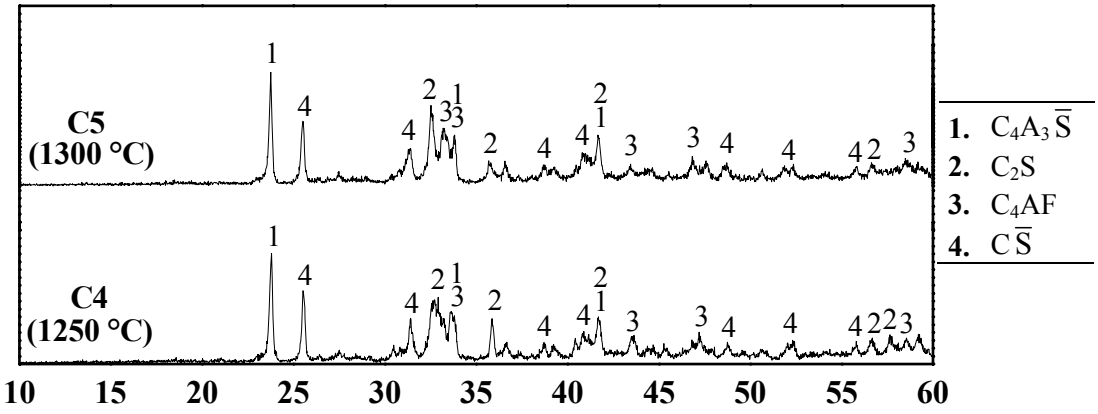


**Figure 4.9:** XRD powder patterns for cements C4 and C5

Comparison of the XRD patterns of two cements with JCPDS line patterns of the expected minerals is illustrated in Figure 4.10.

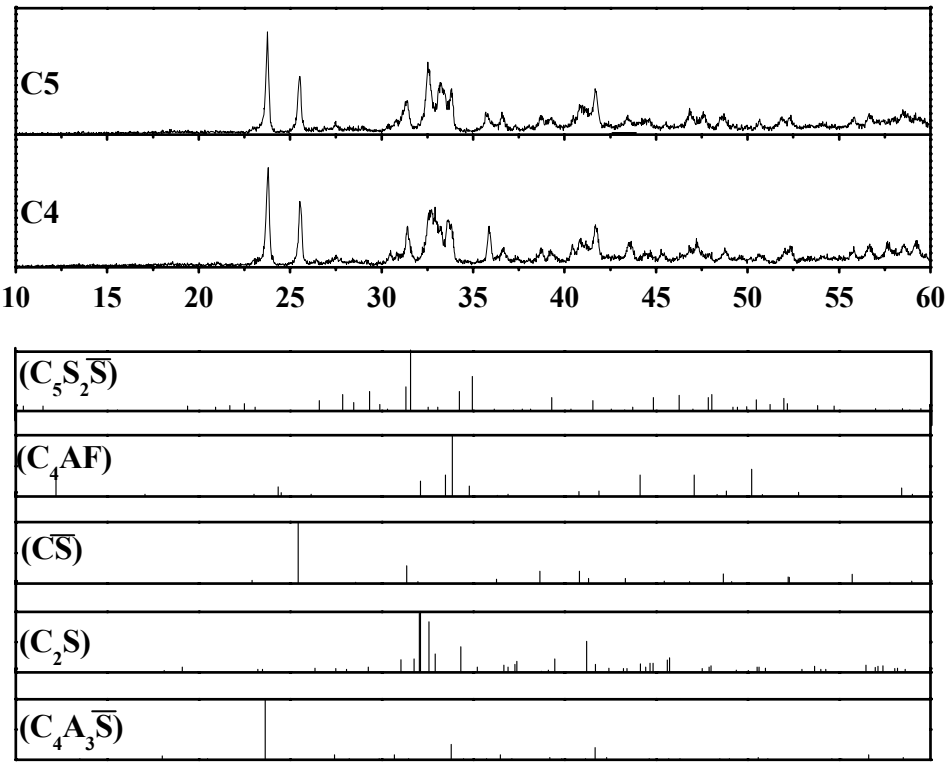


**Figure 4.10:** Comparison of XRD pattern of cements C4 and C5 with standard line patterns of expected minerals

As can be seen from the figures, similar patterns were obtained for both cements C4 and C5 with the formation of $C_4A_3\overline{S}$, β-$C_2S$, $C_4AF$ and $C\overline{S}$. The peaks belonging to $C_5S_2\overline{S}$ mineral were not observed for these two cements. Absence of this mineral present in the cements C1 to C3 obtained for SET 1 is a verification of its decomposition into $C_2S$ and $C\overline{S}$ [40,43]. The presence of the desired minerals and the absence of $C_5S_2\overline{S}$ confirms the formation of the SAB cement at the final sintering temperatures of 1250 °C and 1300 °C for 60 min. The absence of tricalcium aluminate ($C_3A$) mineral in these cements also indicates that the decomposition of the desired mineral $C_4A_3\overline{S}$ did not take place at these temperatures. The highest intensity values of $C_4A_3\overline{S}$ were recorded for cement C4. Intensity values for $C\overline{S}$ are slightly lower for cement C5 than those of cement C4 due to some dissociation of the $C\overline{S}$ at higher temperature.

## 4.7 Scanning Electron Microscopy (SEM)

Microstructure image of the CK4 clinker under scanning electron microscope is shown in Figure 4.11. SEM studies on SAB clinkers indicate that $C_4A_3\overline{S}$ phase appears as cubic or rhombic dodecahedron crystals and $C_2S$ phase appears as rounded grains [28,30,31,50].As can be seen clearly from Figure 4.11 both phases appear well-formed and distinct among the other phases of the clinker. $C_2S$ grains have a size around 1-2 μm while size of $C_4A_3\overline{S}$ crystals changed between 3 to 5 μm.

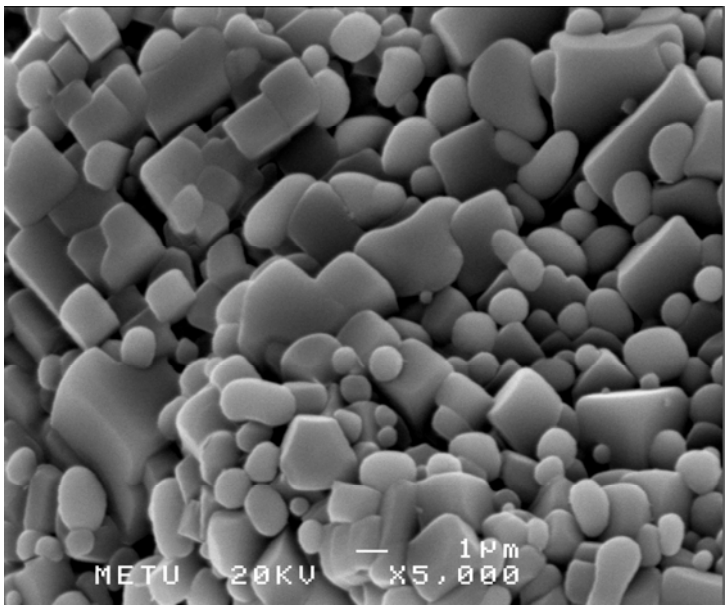


**Figure 4.11:** Scanning electron micrograph of clinker CK4

Figure 4.12 shows the energy dispersive spectrometer (EDS) spot analysis on one of the $C_4A_3\overline{S}$ grains of the clinker CK4. The selected spot is marked with a star. As can be seen from the pattern the main elements present were aluminium, calcium and sulfur. The presence of gold element is obviously due to the thin layer of gold coating. The EDS analysis performed also validates that these structures belong to $C_4A_3\overline{S}$ formation and presence of the calcium sulfoaluminate mineral.

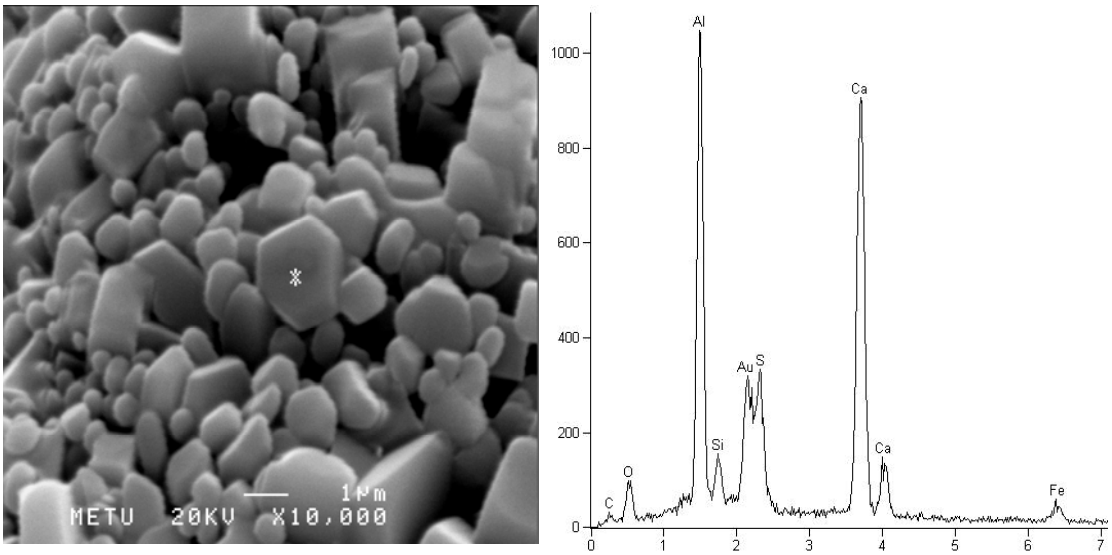


**Figure 4.12:** The EDS-spot analysis of clinker CK4 on the spot marked with a star

# CHAPTER 5

# CONCLUSIONS

## 5.1 General

In this thesis study, utilization potential of FBC ashes as raw material in the production of non-expansive belite-rich calcium sulfoaluminate cement was investigated. The prepared raw meal was subjected to furnace sintering at temperatures of 1200, 1250 and 1300 °C for different holding times. XRD and SEM analysis were performed for mineralogical examination of the obtained samples. The following conclusions were reached under the observations of this study:

- The utilization of FBC ashes by 25 wt % in the raw meal forms the mineral phases of SAB cements, $C_4A_3\overline{S}$, β-$C_2S$, $C_4AF$ and $C\overline{S}$.
- Optimum sintering temperature for the formation of non-expansive belite-rich calcium sulfoaluminate clinker is found to be 1250 °C for the raw meal containing 25 wt % FBC ashes.
- XRD analysis of the clinkers reveals that decomposition of hydraulically inactive undesired phase ternesite ($C_5S_2\overline{S}$) into desired SAB compounds $C_2S$ and $C\overline{S}$ takes place in the clinker obtained at 1250 °C for 60 min.
- The mineral phase $C_4A_3\overline{S}$ is formed at each sintering temperature and remains stable up to temperature of 1300 °C which is verified by the absence of $C_3A$ mineral in the clinkers.

- SEM analysis reveals that the main phases β-$C_2S$ and $C_4A_3\overline{S}$ are rounded grains and cubic or rhombic dodecahedron crystals, respectively.

It is thus concluded that FBC ashes generated from fluidized bed combustion of coal have significant potential for utilization as raw materials in the production of non-expansive belite-rich sulfoaluminate cement.

## 5.2 Suggestions for Future Work

Based on the experience gained in the present study, the following recommendations for future extension of the work are suggested:

- The hydraulic properties of the cements can be investigated by examining the formation and structure of the hydration products.
- Water requirement, compressive strength, setting time and soundness tests with long term durability tests can be performed by producing sufficient amount of samples and the results can be compared with those of OPC.
- Investigations on the quantitative determination of the clinker phases can be performed either using quantitative X-Ray (QXRD) analysis or microscopically.

# REFERENCES


[1] BP Statistical Review of World Energy June 2009
http://www.bp.com/statisticalreview (Last access date: 10.06.2009)

[2] World Coal Institute Coal Facts 2008
http://www.worldcoal.org/pages/content/index.asp?PageID=188
(Last access date: 10.06.2009)

[3] Li F., Zhai J., Fu X. and Sheng G., "Characterization of Fly Ashes from Circulating Fluidized Bed Combustion Boilers Cofiring Coal and Petroleum Coke", *Energy and Fuels*, Vol. 20, 1411-1417, 2006

[4] Selçuk N., "Fluidized Bed Combustion Technologies for Existing Thermal Power Plants", *Turkish Electricity Authority*, 241-254, 1993

[5] Scheetz B.E. and Earle R., "Utilization of Fly Ash", *Current Opinion in Solid State and Materials Science*, Vol. 3, (5) 510-520, 1998

[6] Sajwan K.S., Ashok K. Alva and Robert F., *Chemistry of trace elements in fly ash*, Kluwer Academic/Plenum Publishers, 2003, New York

[7] Coal Combustion Products
http://www.epa.gov/wastes/conserve/rrr/imr/ccps/index.htm
(Last access date: 10.06.2009)

[8] Brown P.W., *Cements research progress*, The American Ceramic Society, 1993

[9] Majling J. and Roy D.M., "The Potential of Fly Ash for Cement Manufacture", *American Ceramic Society Bulletin* Vol. 72, (10) 77-81, 1993

[10] Marroccoli M., Montagnaro F., Nobili M., Telesca A. and Valenti G.L., "Hydration Properties of Calcium Sulphoaluminate Cements made from Coal Combustion Wastes", *30th Meeting on Combustion*, 2007

[11] Belz G., Bernardo G., Caramuscio P., Montagnaro F., Telesca A. and Valenti G.L., "Synthesis of Special Cements from Mixtures Containing Fluidized

Bed Combustion Waste, Calcium Carbonate and Various Sources of Alumina", *28th Meeting of the Italian Section of The Combustion Institute*, 2005

[12] Belz G., Caramuscio P., Marroccoli M., Montagnaro F., Nobili M., Telesca A., and Valenti G.L., "Fluidized Bed Combustion Waste as a Raw Mix Component for the Manufacture of Calcium Sulphoaluminate Cements", *29th Meeting of the Italian Section of The Combustion Institute*, 2006

[13] Gartner E., "Industrially Interesting Approaches to "Low-$CO_2$" Cements", *Cement and Concrete Research*, Vol. 34, 1489-1498, 2004

[14] Bernardo G., Marroccoli M., Montagnaro F. and Valenti G.L., "Calcium Sulphoaluminate Cements made from Fluidized Bed Combustion Wastes", *Waste Materials in Construction: Proceedings of the International Conference on the Science and Engineering of Recycling for Environmental Protection*, 2000

[15] Quillin K., "Performance of Belite-Sulfoaluminate Cements", *Cement and Concrete Research*, Vol. 31, 1341-1349, 2001

[16] Anderson J.E., "Green Cement: Finding a Solution for a Sustainable Cement Industry", *Green Cities Competition Bears Breaking Boundaries Department of Civil and Environmental Engineering*, 2007

[17] Phair J.W., "Green Chemistry for Sustainable Cement Production and Use", *Green Chemistry*, Vol. 8, 763-780, 2006

[18] Pera J. and Ambroise J., "New Applications of Calcium Sulfoaluminate Cement", *Cement and Concrete Research*, Vol. 34, 671-676, 2004

[19] Zhou Q., Milestone N.B. and Hayes M., "An Alternative to Portland Cement for Waste Encapsulation-The Calcium Sulfoaluminate Cement System", *Journal of Hazardous Materials*, Vol. 136, 120-129, 2006

[20] Arjunan P., Silsbee M.R. and Roy D.M., "Sulfoaluminate-Belite Cement from Low-Calcium Fly Ash and Sulfur-Rich and Other Industrial By-Products", *Cement and Concrete Research*, Vol. 29, 1305-1311, 1999

[21] Janotka I., Krajci L. and Mojumdar S.C., "Influence of Portland Cement Addition to Sulphoaluminate-Belite Cement on Hydration and Mechanical

Properties of Hardened Mortars", *Ceramics-Silikaty*, Vol. 46, (3) 110-116, 2002

[22] Sahu S. and Majling J., "Preparation of Sulphoaluminate Belite Cement from Fly Ash", *Cement and Concrete Research*, Vol. 24, (6) 1065-1072, 1994

[23] Beretka J., Marroccoli M., Sherman N. and Valenti G.L., "The Influence of $C_4A_3\overline{S}$ Content and W/S Ratio on the Performance of Calcium Sulfoaluminate-Based Cements", *Cement and Concrete Research*, Vol. 26, (11) 1673-1681, 1996

[24] Janotka I., Krajci L. and Mojumdar S.C., "Performance of Sulphoaluminate-Belite Cements with High $C_4A_3\overline{S}$ Content", *Ceramics-Silikaty*, Vol. 51, (2) 74-81, 2007

[25] Adolfsson D., Menad N., Viggh E. and Björkman B., "Steelmaking Slags as Raw Material for Sulphoaluminate Belite Cement", *Advances in Cement Research*, Vol. 19, (4) 147-156, 2007

[26] Popescu C.D., Muntean M. and Sharp J.H., "Industrial Trial Production of Low Energy Belite Cement", *Cement and Concrete Composites*, Vol. 25, 689-693, 2003

[27] Glasser F.P. and Zhang L., "High-Performance Cement Matrices Based on Calcium Sulfoaluminate-Belite Compositions", *Cement and Concrete Research*, Vol. 31, 1881-1886, 2001

[28] Katsioti M., Tsakiridis P.E., Leonardou-Agatzini S. and Oustadakis P., "Examination of the Jarosite-Alunite Precipitate Addition in the Raw Meal for the Production of Sulfoaluminate Cement Clinker", *Journal of Hazardous Materials*, Vol. 131, (1-3) 187-194, 2006

[29] Kasselouri V., Tsakiridis P., Malami C., Georgali B. and Alexandridou C., "A Study on the Hydration Products of a Non-Expansive Sulfoaluminate Cement", *Cement and Concrete Research*, Vol. 25, (8) 1726-1736, 1995

[30] Mehta P.K., "Investigations on Energy-saving Cements", *World Cement Technology*, Vol. 11, (5) 166-177, 1980

[31] Bogue R.H., *The Chemistry of Portland Cement*, *2nd ed.*, Reinhold Publishing Corporation, New York, 1955

[32] EN 197-1, *Cement-Part1: Composition, specifications and conformity criteria for common cements*, European Committee for Standardization, 2000

[33] Megnin L.L., "Cement Manufacturing", *Lubrication Magazine*, Vol. 86, (5) 2002

[34] Lea F.M. and Hewlett P.C., *Lea's Chemistry of Cement and Concrete*,*4th ed*, 2004

[35] Ramachandran V.S., *Handbook of Analytic Techniques in Concrete Science and Technology*, Noyes Publications / William Andrew Publishing, 2001

[36] Kosmatka S., Kerkhoff B. and Panarese W., *Design and Control of Concrete Mixtures*,*14th ed*,Portland Cement Association, 2002

[37] Taylor H.F.W., *Cement Chemistry*, *2nd ed*, Academic Press, London, 1990

[38] Erdoğan T.Y., *Beton*,*1st ed*,Metu Press, 2003

[39] Labahn O. and Kohlhaas B., *Cement Engineer's Handbook*,*4rd ed*, 1983

[40] Odler I., *Special inorganic cements*, *1st ed*, Taylor and Francis, 2000

[41] Mehta P.K., "Mechanism of Expansion Associated with Ettringite Formation", *Cement and Concrete Composites*, Vol. 3, 1-6, 1973

[42] Kalogridis D., Kostogloudis G.C., Ftikos C. and Malami C., "A Quantitative Study of the Influence of Non-Expansive Sulfoaluminate Cement on the Corrosion of Steel Reinforcement", *Cement and Concrete Research*, Vol. 30, 1731-1740, 2000

[43] Roy D.M., Silsbee M.R. and Xie Z., "Influences of Surplus $SO_3$ in FBC Ash on Formation of Belite-Rich Sulfoaluminate Clinker", *International Ash Utilization Symposium*, 1999

[44] Duda W.H., *Cement-Data-Book*,*2nd ed*,Macdonald and Evans, London, 1977

[45] Zhang L. and Glasser F.P., "Hydration of Calcium Sulfoaluminate Cement at less than 24 h", *Advances in Cement Research*, Vol. 14, (4) 141-155, 2002

[46] Uchikawa H., "Management Strategy in Cement Technology for the Next Century part 3", *World Cement*, 47-54 November, 1994

[47] Teoreanu I. and Muntean M., "Expansive Sulphate Aluminate Cements", *Cement and Concrete Research*, Vol. 13, 711-720, 1983

[48] Jewell R.B., Rathbone R.F. and Robl T.L., "The Fabrication of Value Added Cement Products from Circulating Fluidized Bed Combustion Ash", *World of Coal Ash (WOCA) Covington, Kentucky, USA*, 2007

[49] Gogebakan Z., Gogebakan Y. and Selçuk N., "Co-Firing of Olive Residue with Lignite in Bubbling FBC", *Combustion Science and Technology*, Vol. 180, 854-868, 2008

[50] Chang J., Lu L., Huang S., Liu F., Wang Z. and Cheng X., "Industrial production of Ba-bearing Sulphoaluminate Cement", *Advances in Cement Research*, Vol. 18, (1) 41-45, 2006

[51] Ali M.M., Gopal S. and Handoo S.K., "Studies on the Formation Kinetics of Calcium Sulphoaluminate", *Cement and Concrete Research*, Vol. 24, (4) 715-720, 1994

[52] Beretka J., Vito B., Santoro L., Sherman N. and Valenti G.L., "Hydraulic Behaviour of Calcium Sulfoaluminate-Based Cements Derived from Industrial Process Wastes", *Cement and Concrete Research*, Vol. 23, 1205-1214, 1993

[53] Gies A. and Knofel D., "Influence of Alkalies on the Composition of Belite-Rich Cement Clinkers and the Technological Properties of the Resulting Cements", *Cement and Concrete Research*, Vol. 16, 411-422, 1986

[54] Singh M., Kapur P.C. and Pradip, "Preparation of Calcium Sulphoaluminate Cement Using Fertiliser Plant Wastes", *Journal of Hazardous Materials*, Vol. 157, 106-113, 2008

[55] Shih P.-H., Chang J.-E. and Chiang L.-C., "Replacement of raw mix in cement production by municipal solid waste incineration ash", *Cement and Concrete Research*, Vol. 33, 1831-1836, 2003

[56] Jones R., "Successful Particle Size Analysis of Dry Powders", *Process Analytics*, Vol. 2, 46-48, 2002

[57] Particle Size Analysis and the Use of Laser Diffraction on Small Sample Volumes Using Equipment From Malvern Instruments
http://www.azom.com/Details.asp?ArticleID=2816
(Last access date: 05.06.2009)

[58] Kürkçü M., “Utilization of fly ash from fluidized bed combustion of a Turkish lignite in production of blended cements” Master Thesis, 2006

[59] Espinosa D.C.R. and Tenorio J.A.S., "Laboratory study of galvanic sludge’s influence on the clinkerization process", *Resources, Conservation and Recycling* Vol. 31, 71-82, 2000

[60] Caponero J. and Tenorio J.A.S., "Laboratory testing of the use of phosphate-coating sludge in cement clinker", *Resources, Conservation and Recycling*, Vol. 29, 169-179, 2000

[61] Sherman N., Beretka J., Santoro L. and Valenti G.L., "Long-Term Behaviour of Hydraulic Binders Based on Calcium Sulfoaluminate and Calcium Sulfosilicate", *Cement and Concrete Research*, Vol. 25, (1) 113-126, 1995

# APPENDIX A

# MODIFIED BOGUE CALCULATION (POTENTIAL CEMENT COMPOSITION)

The potential mineralogical composition of the cement can be determined approximately by using the chemical analysis of the cement. This phase calculation, universally known as *Bogue calculation,* yields reasonably approximate values for guidance.

The modified Bogue formulas for calcium sulfoaluminate based cements were derived by considering the following assumptions [34,37,39]:

- The cement is entirely crystalline, no glass remains in the clinker after cooling
- Clinker melt (liquid phase in clinkering) crystallizes in equilibrium with the solid phases
- The mineral phases are chemically pure and stoichiometric composition, i.e. pure $C_4A_3\overline{S}$, $C_2S$, $C_4AF$ and $C\overline{S}$

The main components (C, S, A, F) present in cement under equilibrium conditions is approximately assumed to be combined as follows [20,21,25,29,30,31,37]:

1. All the "F" present is combined as $C_4AF$
2. All the "S" present is combined as $C_2S$
3. The remaining "A", which is calculated by subtracting the amount of "A" present in $C_4AF$ from total "A" content, is combined as $C_4A_3\overline{S}$
4. The remaining "$\overline{S}$", which is calculated by subtracting the amount of "$\overline{S}$"present in $C_4A_3\overline{S}$ from total "$\overline{S}$", is combined as $C\overline{S}$

where the cement notations in quotation marks refer to chemical composition values in cement. This procedure can be formulated sequentially,

**1.** $\%\ C_4AF = (\%\ F)\ x \left( \frac{MW_{C_4AF}}{MW_F} \right)$

$\%\ C_4AF = (\%\ F)\ x \left( \frac{486}{160} \right)$

**$\%\ C_4AF = 3.043\ x\ (\%\ F)$**

**2.** $\%\ C_2S = (\%\ S)\ x \left( \frac{MW_{C_2S}}{MW_S} \right)$

$\%\ C_2S = (\%\ S)\ x \left( \frac{172}{60} \right)$

**$\%\ C_2S = 2.87\ x\ (\%\ S)$**

**3.** $\%\ C_4A_3\overline{S} = \left( \%\ A - \%\ C_4AF\ x\ \frac{MW_A}{MW_{C_4AF}} \right) x\ \frac{MW_{C_4A_3\overline{S}}}{3\ x\ MW_A}$

$\%\ C_4A_3\overline{S} = \left( \%\ A - \mathbf{3.043\ x}\ (\%\ \mathbf{F})\ x\ \frac{102}{486} \right) x\ \frac{602}{3\ x\ 102}$

**$\%\ C_4A_3\overline{S} = 1.97\ x\ (\%\ A) - 1.26\ x\ (\%\ F)$**

**4.** $\%\ C\overline{S} = \left( \%\ \overline{S} - \%\ C_4A_3\overline{S}\ x\ \frac{MW_{\overline{S}}}{MW_{C_4A_3\overline{S}}} \right) x\ \frac{MW_{C\overline{S}}}{MW_{\overline{S}}}$

$\%\ C\overline{S} = \left( \%\ \overline{S} - \left( \mathbf{1.97\ x}\ (\%\ \mathbf{A}) - \mathbf{1.26\ x}\ (\%\ \mathbf{F}) \right) x\ \frac{80}{602} \right) x\ \frac{136}{80}$

**$\%\ C\overline{S} = 1.7\ x\ (\%\ \overline{S}) - 0.45\ x\ (\%\ A) + 0.285\ x\ (\%\ F)$**

# APPENDIX B

# HEATING PROFILES OF SETS

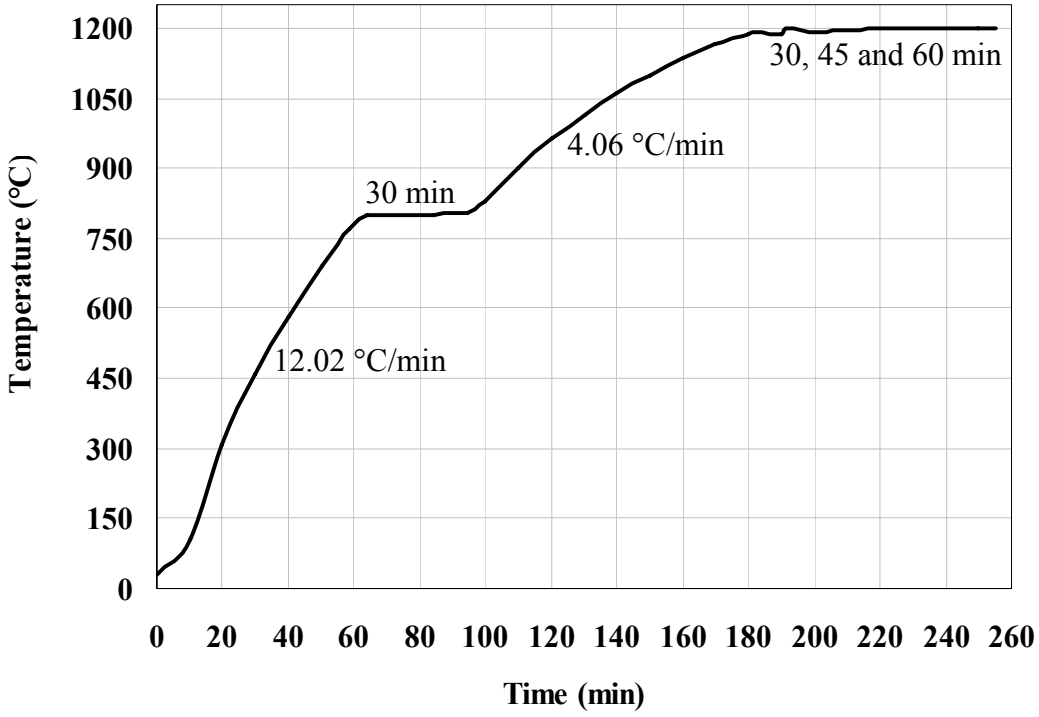


**Figure B.1:** Heating profile for SET 1

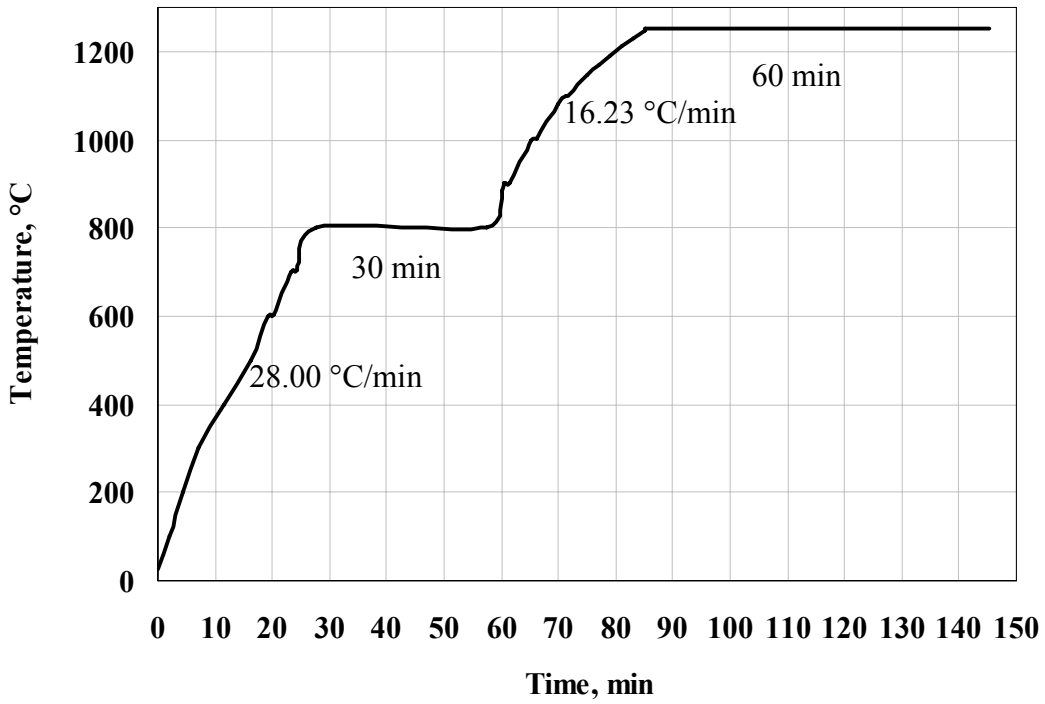


**Figure B.2:** Heating profile for SET 2

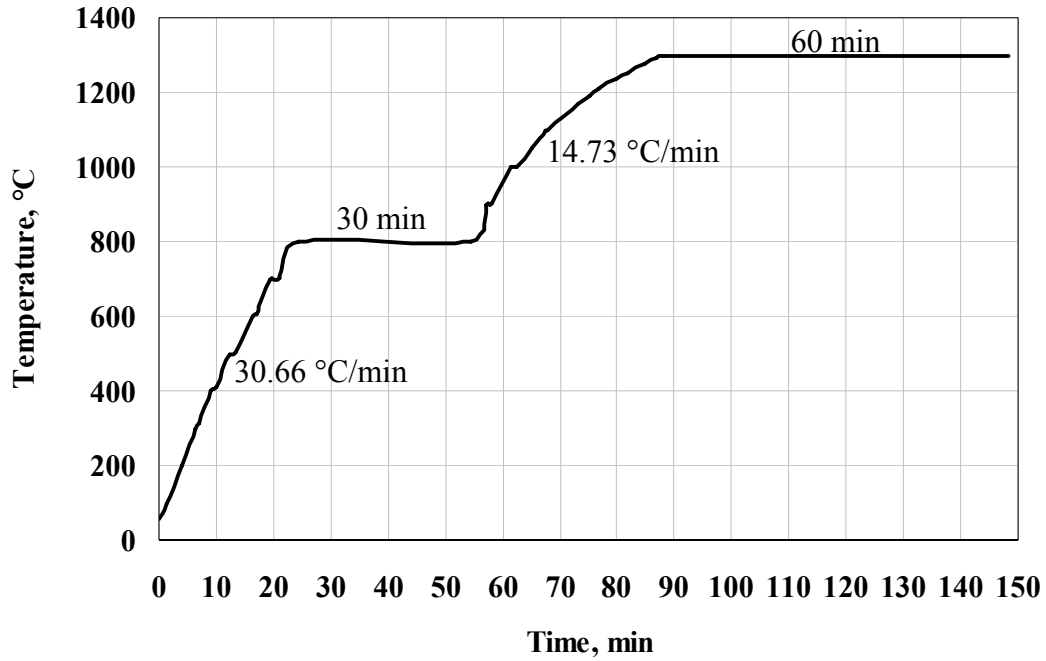


**Figure B.3:** Heating profile for SET 3

# APPENDIX C

# TABULATED PARTICLE SIZE DISTRIBUTIONS

**Table C.1:** Particle size distribution of limestone

| Size, µm | Cumulative Weight, % | Size, µm | Cumulative Weight, % |
|---|---|---|---|
| 178.250 | 0.000 | 5.637 | 44.980 |
| 158.866 | 0.050 | 5.024 | 46.670 |
| 141.589 | 0.200 | 4.477 | 48.380 |
| 126.191 | 0.600 | 3.991 | 50.140 |
| 112.468 | 1.240 | 3.557 | 51.940 |
| 100.237 | 2.170 | 3.170 | 53.810 |
| 89.337 | 3.380 | 2.825 | 55.760 |
| 79.621 | 4.850 | 2.518 | 57.780 |
| 70.963 | 6.530 | 2.244 | 59.880 |
| 63.246 | 8.370 | 2.000 | 62.080 |
| 56.368 | 10.290 | 1.783 | 64.360 |
| 50.238 | 12.230 | 1.589 | 66.740 |
| 44.774 | 14.170 | 1.416 | 69.230 |
| 39.905 | 16.060 | 1.262 | 71.850 |
| 35.566 | 17.890 | 1.125 | 74.600 |
| 31.698 | 19.670 | 1.002 | 77.490 |
| 28.251 | 21.410 | 0.893 | 80.480 |
| 25.179 | 23.120 | 0.796 | 83.520 |
| 22.440 | 24.800 | 0.710 | 86.530 |
| 20.000 | 26.480 | 0.632 | 89.420 |
| 17.825 | 28.160 | 0.564 | 92.120 |
| 15.887 | 29.840 | 0.502 | 94.510 |
| 14.159 | 31.530 | 0.448 | 96.550 |
| 12.619 | 33.230 | 0.399 | 98.140 |
| 11.247 | 34.930 | 0.356 | 99.290 |
| 10.024 | 36.620 | 0.317 | 99.950 |
| 8.934 | 38.300 | 0.283 | 100.000 |
| 7.962 | 39.980 | | |
| 7.096 | 41.650 | | |
| 6.325 | 43.310 | | |

**Table C.2:** Particle size distribution of bottom ash

| Size, µm | Cumulative Weight, % | Size, µm | Cumulative Weight, % |
|---|---|---|---|
| 158.866 | 0.000 | 2.518 | 87.020 |
| 141.589 | 0.530 | 2.244 | 88.210 |
| 126.191 | 2.540 | 2.000 | 89.310 |
| 112.468 | 5.340 | 1.783 | 90.320 |
| 100.237 | 8.870 | 1.589 | 91.240 |
| 89.337 | 12.830 | 1.416 | 92.090 |
| 79.621 | 16.960 | 1.262 | 92.890 |
| 70.963 | 21.060 | 1.125 | 93.650 |
| 63.246 | 24.990 | 1.002 | 94.410 |
| 56.368 | 28.670 | 0.893 | 95.180 |
| 50.238 | 32.110 | 0.796 | 95.950 |
| 44.774 | 35.320 | 0.710 | 96.710 |
| 39.905 | 38.350 | 0.632 | 97.450 |
| 35.566 | 41.260 | 0.564 | 98.140 |
| 31.698 | 44.100 | 0.502 | 98.760 |
| 28.251 | 46.870 | 0.448 | 99.280 |
| 25.179 | 49.600 | 0.399 | 99.680 |
| 22.440 | 52.280 | 0.356 | 99.910 |
| 20.000 | 54.870 | 0.317 | 99.990 |
| 17.825 | 57.380 | 0.283 | 100.000 |
| 15.887 | 59.780 | | |
| 14.159 | 62.070 | | |
| 12.619 | 64.240 | | |
| 11.247 | 66.310 | | |
| 10.024 | 68.270 | | |
| 8.934 | 70.140 | | |
| 7.962 | 71.930 | | |
| 7.096 | 73.660 | | |
| 6.325 | 75.330 | | |
| 5.637 | 76.950 | | |
| 5.024 | 78.530 | | |
| 4.477 | 80.070 | | |
| 3.991 | 81.570 | | |
| 3.557 | 83.020 | | |
| 3.170 | 84.420 | | |
| 2.825 | 85.750 | | |

**Table C.3:** Particle size distribution of baghouse filter ash

| Size, µm | Cumulative Weight, % | Size, µm | Cumulative Weight, % |
|---|---|---|---|
| 39.905 | 0.000 | 0.632 | 97.050 |
| 35.566 | 0.010 | 0.564 | 97.900 |
| 31.698 | 0.070 | 0.502 | 98.660 |
| 28.251 | 0.180 | 0.448 | 99.270 |
| 25.179 | 0.370 | 0.399 | 99.710 |
| 22.440 | 0.680 | 0.356 | 99.940 |
| 20.000 | 1.170 | 0.317 | 99.990 |
| 17.825 | 1.890 | 0.283 | 100.000 |
| 15.887 | 2.950 | | |
| 14.159 | 4.470 | | |
| 12.619 | 6.620 | | |
| 11.247 | 9.520 | | |
| 10.024 | 13.290 | | |
| 8.934 | 18.000 | | |
| 7.962 | 23.610 | | |
| 7.096 | 30.030 | | |
| 6.325 | 37.050 | | |
| 5.637 | 44.420 | | |
| 5.024 | 51.840 | | |
| 4.477 | 59.000 | | |
| 3.991 | 65.640 | | |
| 3.557 | 71.570 | | |
| 3.170 | 76.630 | | |
| 2.825 | 80.800 | | |
| 2.518 | 84.120 | | |
| 2.244 | 86.670 | | |
| 2.000 | 88.580 | | |
| 1.783 | 89.980 | | |
| 1.589 | 91.010 | | |
| 1.416 | 91.800 | | |
| 1.262 | 92.480 | | |
| 1.125 | 93.110 | | |
| 1.002 | 93.770 | | |
| 0.893 | 94.490 | | |
| 0.796 | 95.300 | | |
| 0.710 | 96.160 | | |

**Table C.4:** Particle size distribution of bauxite

| Size, µm | Cumulative Weight, % | Size, µm | Cumulative Weight, % |
|---|---|---|---|
| 709.627 | 0.000 | 11.247 | 87.580 |
| 632.456 | 0.030 | 10.024 | 88.560 |
| 563.677 | 0.110 | 8.934 | 89.420 |
| 502.377 | 0.240 | 7.962 | 90.160 |
| 447.744 | 0.390 | 7.096 | 90.810 |
| 399.052 | 0.550 | 6.325 | 91.370 |
| 355.656 | 0.720 | 5.637 | 91.860 |
| 316.979 | 0.910 | 5.024 | 92.300 |
| 282.508 | 1.170 | 4.477 | 92.700 |
| 251.785 | 1.530 | 3.991 | 93.060 |
| 224.404 | 2.100 | 3.557 | 93.400 |
| 200.000 | 3.000 | 3.170 | 93.710 |
| 178.250 | 4.390 | 2.825 | 94.010 |
| 158.866 | 6.390 | 2.518 | 94.280 |
| 141.589 | 9.110 | 2.244 | 94.530 |
| 126.191 | 12.610 | 2.000 | 94.770 |
| 112.468 | 16.850 | 1.783 | 94.980 |
| 100.237 | 21.740 | 1.589 | 95.190 |
| 89.337 | 27.120 | 1.416 | 95.390 |
| 79.621 | 32.790 | 1.262 | 95.620 |
| 70.963 | 38.540 | 1.125 | 95.870 |
| 63.246 | 44.190 | 1.002 | 96.180 |
| 56.368 | 49.560 | 0.893 | 96.530 |
| 50.238 | 54.560 | 0.796 | 96.930 |
| 44.774 | 59.120 | 0.710 | 97.370 |
| 39.905 | 63.240 | 0.632 | 97.840 |
| 35.566 | 66.930 | 0.564 | 98.310 |
| 31.698 | 70.220 | 0.502 | 98.760 |
| 28.251 | 73.150 | 0.448 | 99.170 |
| 25.179 | 75.760 | 0.399 | 99.520 |
| 22.440 | 78.090 | 0.356 | 99.790 |
| 20.000 | 80.180 | 0.317 | 99.980 |
| 17.825 | 82.040 | 0.283 | 100.000 |
| 15.887 | 83.690 | | |
| 14.159 | 85.160 | | |
| 12.619 | 86.450 | | |

**Table C.5:** Particle size distribution of gypsum

| Size, µm | Cumulative Weight, % | Size, µm | Cumulative Weight, % |
|---|---|---|---|
| 70.963 | 0.000 | 1.125 | 83.470 |
| 63.246 | 0.100 | 1.002 | 85.810 |
| 56.368 | 0.270 | 0.893 | 87.980 |
| 50.238 | 0.550 | 0.796 | 89.990 |
| 44.774 | 0.860 | 0.710 | 91.820 |
| 39.905 | 1.180 | 0.632 | 93.480 |
| 35.566 | 1.480 | 0.564 | 94.950 |
| 31.698 | 1.750 | 0.502 | 96.230 |
| 28.251 | 1.980 | 0.448 | 97.320 |
| 25.179 | 2.210 | 0.399 | 98.200 |
| 22.440 | 2.460 | 0.356 | 98.880 |
| 20.000 | 2.870 | 0.317 | 99.360 |
| 17.825 | 3.540 | 0.283 | 99.710 |
| 15.887 | 4.560 | 0.252 | 99.950 |
| 14.159 | 5.990 | 0.224 | 100.000 |
| 12.619 | 7.870 | | |
| 11.247 | 10.240 | | |
| 10.024 | 13.060 | | |
| 8.934 | 16.310 | | |
| 7.962 | 19.920 | | |
| 7.096 | 23.830 | | |
| 6.325 | 27.960 | | |
| 5.637 | 32.260 | | |
| 5.024 | 36.640 | | |
| 4.477 | 41.060 | | |
| 3.991 | 45.440 | | |
| 3.557 | 49.750 | | |
| 3.170 | 53.940 | | |
| 2.825 | 57.980 | | |
| 2.518 | 61.850 | | |
| 2.244 | 65.530 | | |
| 2.000 | 69.010 | | |
| 1.783 | 72.280 | | |
| 1.589 | 75.360 | | |
| 1.416 | 78.250 | | |
| 1.262 | 80.950 | | |

**Table C.6:** Particle size distribution of raw meal

| Size, µm | Cumulative Weight, % | Size, µm | Cumulative Weight, % |
|---|---|---|---|
| 158.866 | 0.000 | 2.825 | 61.730 |
| 141.589 | 0.030 | 2.518 | 64.640 |
| 126.191 | 0.090 | 2.244 | 67.570 |
| 112.468 | 0.240 | 2.000 | 70.510 |
| 100.237 | 0.540 | 1.783 | 73.400 |
| 89.337 | 1.030 | 1.589 | 76.220 |
| 79.621 | 1.750 | 1.416 | 78.920 |
| 70.963 | 2.730 | 1.262 | 81.480 |
| 63.246 | 3.980 | 1.125 | 83.880 |
| 56.368 | 5.510 | 1.002 | 86.110 |
| 50.238 | 7.290 | 0.893 | 88.170 |
| 44.774 | 9.270 | 0.796 | 90.050 |
| 39.905 | 11.420 | 0.710 | 91.770 |
| 35.566 | 13.670 | 0.632 | 93.320 |
| 31.698 | 15.970 | 0.564 | 94.720 |
| 28.251 | 18.260 | 0.502 | 95.950 |
| 25.179 | 20.490 | 0.448 | 97.030 |
| 22.440 | 22.630 | 0.399 | 97.940 |
| 20.000 | 24.670 | 0.356 | 98.690 |
| 17.825 | 26.620 | 0.317 | 99.260 |
| 15.887 | 28.490 | 0.283 | 99.690 |
| 14.159 | 30.310 | 0.252 | 99.900 |
| 12.619 | 32.120 | 0.224 | 100.000 |
| 11.247 | 33.930 | | |
| 10.024 | 35.780 | | |
| 8.934 | 37.680 | | |
| 7.962 | 39.650 | | |
| 7.096 | 41.700 | | |
| 6.325 | 43.850 | | |
| 5.637 | 46.100 | | |
| 5.024 | 48.440 | | |
| 4.477 | 50.900 | | |
| 3.991 | 53.460 | | |
| 3.557 | 56.130 | | |
| 3.170 | 58.890 | | |

# APPENDIX D

# FREQUENCY CURVES

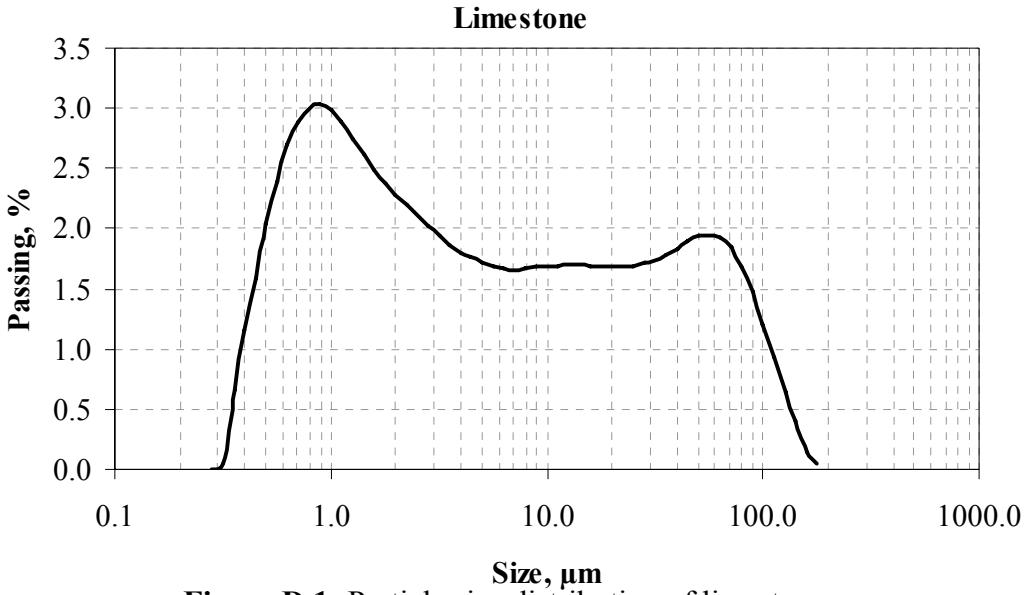


**Figure D.1:** Particle size distribution of limestone

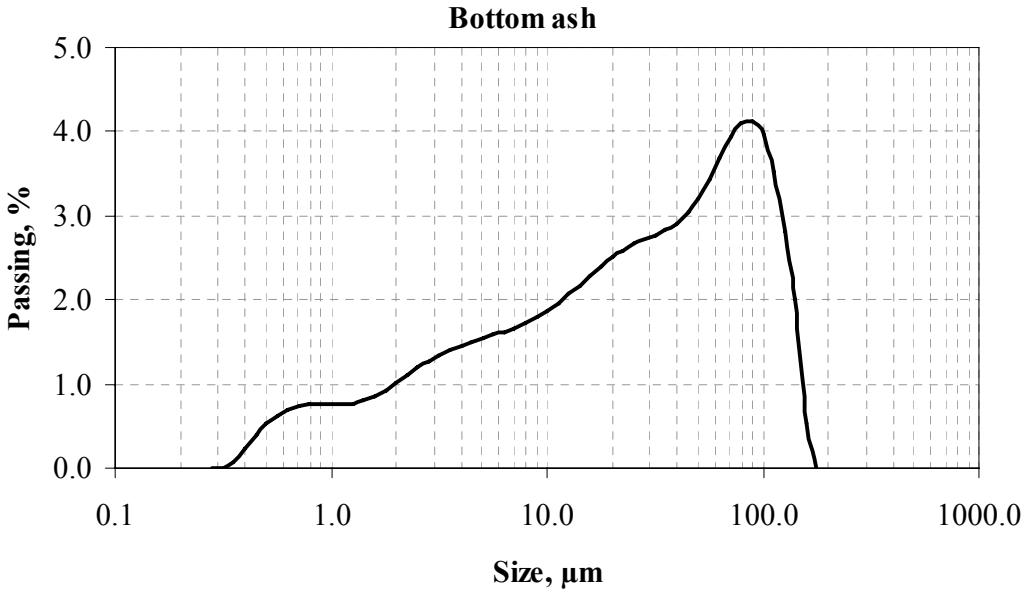


**Figure D.2:** Particle size distribution of bottom ash

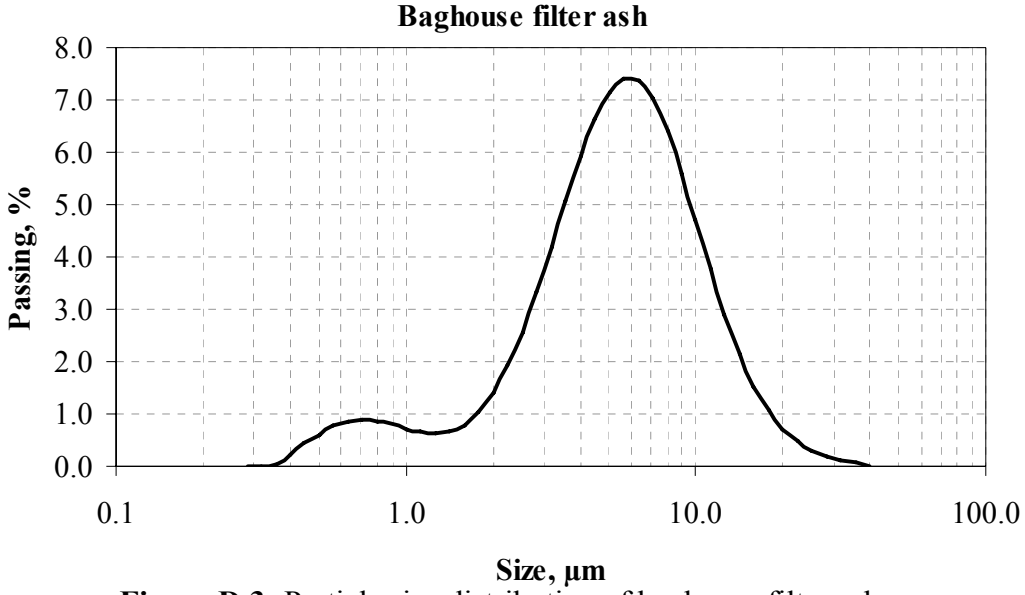


**Figure D.3:** Particle size distribution of baghouse filter ash

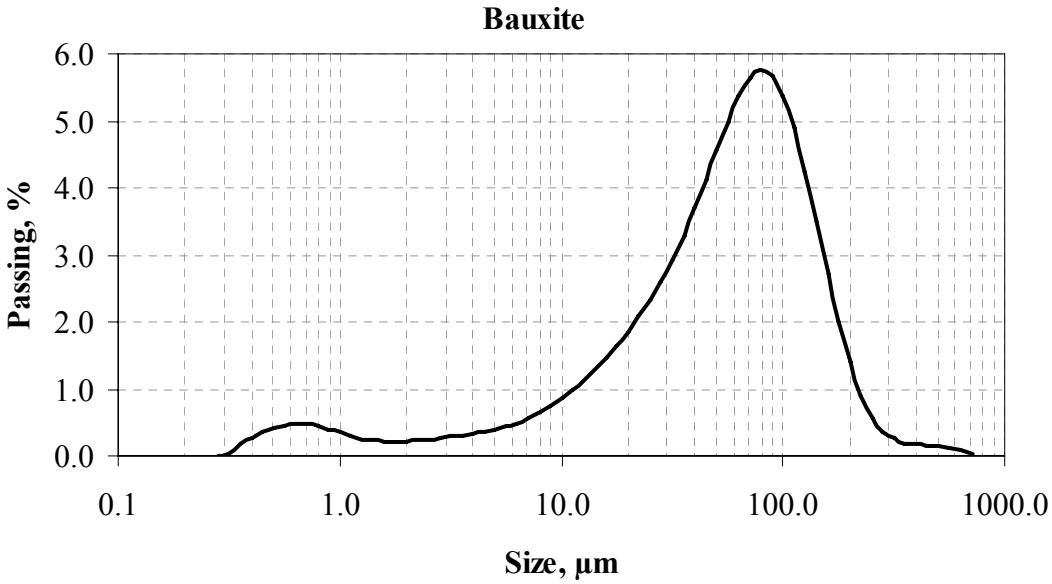


**Figure D.4:** Particle size distribution of bauxite

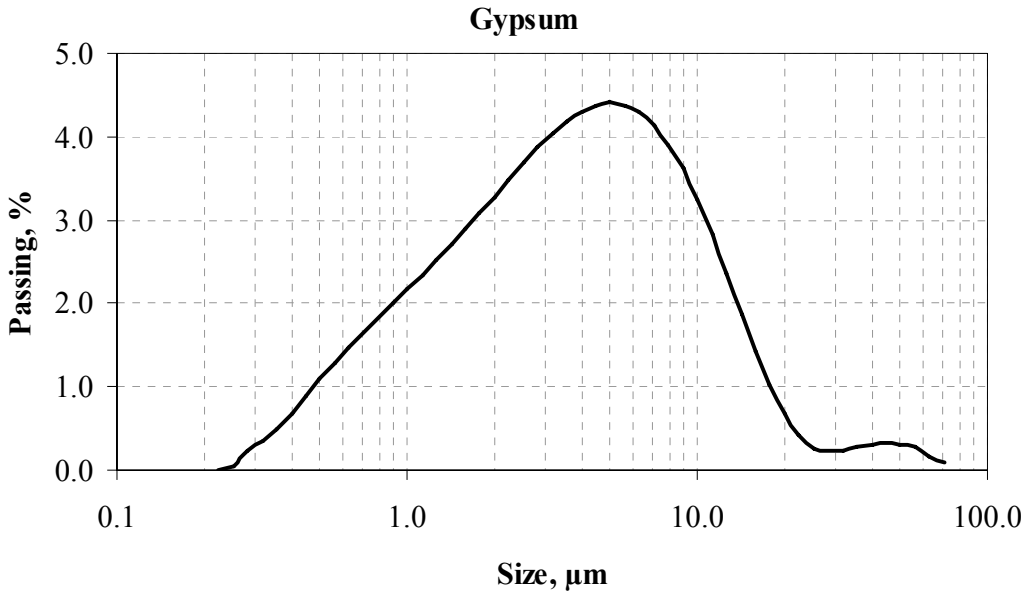


**Figure D.5:** Particle size distribution of gypsum

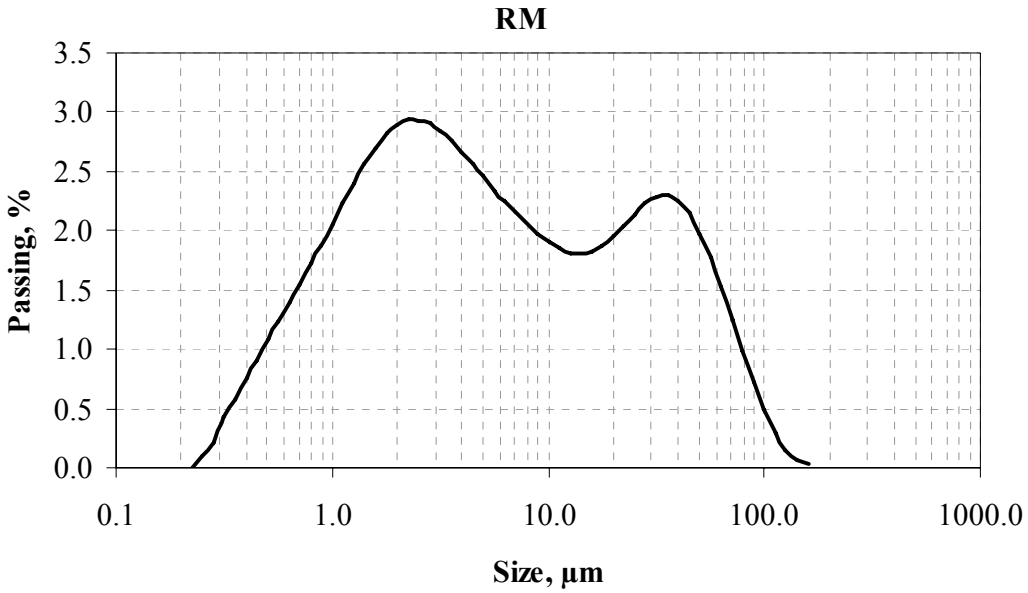


**Figure D.6:** Particle size distribution of raw meal, RM

# APPENDIX E

# DETERMINATION OF MINERAL PHASES

Each crystalline mineral has a distinctive pattern with characteristic interplanar spacings, d-values, which can be obtained with Bragg's law, Equation (E.1), by using measured angle between the incident beam and the normal to the reflecting lattice plane, Θ.

$$n.\lambda = 2.d.\sin(\Theta) \qquad (E.1)$$

Crystalline minerals of the cements were identified by comparing the peak data with the Joint Committee on Powder Diffraction Standards (JCPDS) data of possible expected minerals to be formed. It is appropriate to use diffraction angles, 2Θ, for comparison purpose since the wavelength of X-radiation, λ, used for the analysis of cements in the experiments is same with that of JCPDS data. Therefore, 2Θ values and relative intensities of the peak points with those of possible cementitious minerals are tabulated here. There are small shifts in peak points when compared with pure synthetic minerals. Some peak points correspond to more than one mineral which cause overlapped peaks. Highlighted peak values show possible minerals belong to peak points of the XRD patterns of the cements.

**Table E.1:** Comparison of 2Θ values of peak points of C1 with standard 2Θ values of expected minerals with corresponding relative intensities

| Cement | | Possible cementitious minerals | | | | |
|---|---|---|---|---|---|---|
| C1 | | Yeelimite (33-0256) | Larnite (33-0302) | Anhydrite (37-1496 ) | Brownmillerite (30-0226 ) | Ternesite (49-1807) |
| 2Θ | R.I. | 2Θ (R.I.) | 2Θ (R.I.) | 2Θ (R.I.) | 2Θ (R.I.) | 2Θ (R.I.) |
| 19.480 | 20 | | 19.108 (9) | | 12.198 (45) | 19.389 (8) |
| 21.840 | 15 | | | | | |
| 22.600 | 22 | | | | | 22.494 (12) |
| 23.780 | 76 | 23.643(100) | | | 24.339 (16) | |
| 25.540 | 26 | | | 25.436(100) | | |
| 26.760 | 32 | | | | | 26.594 (17) |
| 28.000 | 50 | | | | | 27.874 (27) |
| 28.620 | 22 | | | | | 28.469 (14) |
| 29.460 | 30 | | 29.267 (9) | | | 29.334 (32) |
| 30.000 | 29 | | | | | 29.914 (11) |
| | | | 31.059 (21) | | | |
| 31.480 | 100 | | | 31.367 (29) | | 31.324 (40) |
| 31.680 | 85 | | | | | 31.584(100) |
| | | | 31.773 (22) | | | |
| | | | 32.054 (97) | | 32.124 (25) | |
| | | | 32.136(100) | | | |
| | | | 32.593 (83) | | | |
| | | | 32.926 (30) | | | |
| 33.480 | 28 | | | | 33.497 (35) | |
| 33.840 | 35 | 33.796 (25) | | | 33.875 (100) | |
| 34.360 | 42 | | 34.330 (42) | | | 34.239 (32) |
| 35.020 | 50 | | | | 34.798 (17) | 34.949 (57) |
| 35.900 | 38 | | 35.235 (9) | | | |
| | | | 36.680 (12) | 38.640 (20) | | |
| | | | 37.280 (13) | | | |
| | | | 37.392 (18) | | | |
| 39.420 | 22 | | 39.473 (22) | | | 39.299 (22) |
| 40.900 | 16 | | | 40.815 (20) | | |
| 41.660 | 43 | 41.663 (20) | 41.206 (51) | | | 41.534 (17) |
| | | | 41.683 (13) | | | |
| 43.520 | 20 | | | 43.330 (8) | | |
| 43.960 | 20 | | 44.141 (14) | | 44.118 (35) | |
| | | | 44.669 (15) | | | |
| 44.940 | 22 | | 44.832 (15) | | | 44.849 (22) |
| | | | 45.618 (20) | | | |
| 46.340 | 37 | | 45.740 (24) | | | 46.254 (26) |
| | | | | | 47.089 (35) | 47.859 (22) |
| 48.080 | 55 | | 48.008 (11) | 48.674 (16) | | 48.039 (27) |

**Table E.2:** Comparison of 2Θ values of peak points of C2 with standard 2Θ values of expected minerals with corresponding relative intensities

| Cement | | Possible cementitious minerals | | | | |
|---|---|---|---|---|---|---|
| C2 | | Yeelimite (33-0256) | Larnite (33-0302) | Anhydrite (37-1496 ) | Brownmillerite (30-0226 ) | Ternesite (49-1807) |
| 2Θ | R.I. | 2Θ (R.I.) | 2Θ (R.I.) | 2Θ (R.I.) | 2Θ (R.I.) | 2Θ (R.I.) |
| 19.500 | 17 | | 19.108 (9) | | 12.198 (45) | 19.389 (8) |
| 21.840 | 17 | | | | | |
| 22.600 | 25 | | | | | 22.494 (12) |
| 23.780 | 81 | 23.643 (100) | | | 24.339 (16) | |
| 25.540 | 28 | | | 25.436 (100) | | |
| 26.760 | 27 | | | | | 26.594 (17) |
| 28.000 | 53 | | | | | 27.874 (27) |
| 28.620 | 26 | | | | | 28.469 (14) |
| 29.460 | 33 | | 29.267 (9) | | | 29.334 (32) |
| 30.000 | 31 | | | | | 29.914 (11) |
| 30.480 | 18 | | 31.059 (21) | | | 31.324 (40) |
| 31.480 | 100 | | | 31.367 (29) | | 31.584(100) |
| | | | 31.773 (22) | | | |
| 31.680 | 87 | | 32.054 (97) | | | |
| | | | 32.136(100) | | 32.124 (25) | |
| | | | 32.593 (83) | | | |
| | | | 32.926 (30) | | | |
| 33.500 | 31 | | | | 33.497 (35) | |
| 33.860 | 48 | 33.796 (25) | | | 33.875 (100) | |
| 34.340 | 43 | | 34.330 (42) | | | 34.239 (32) |
| 35.040 | 50 | | | | 34.798 (17) | 34.949 (57) |
| 35.920 | 40 | | 35.235 (9) | | | |
| | | | 36.680 (12) | 38.640 (20) | | |
| | | | 37.280 (13) | | | |
| | | | 37.392 (18) | | | |
| 39.400 | 28 | | 39.473 (22) | | | 39.299 (22) |
| 40.860 | 15 | | | 40.815 (20) | | |
| 41.680 | 54 | 41.663 (20) | 41.206 (51) | | | 41.534 (17) |
| | | | 41.683 (13) | | | |
| 43.640 | 20 | | | 43.330 (8) | | |
| 43.960 | 19 | | 44.141 (14) | | 44.118 (35) | |
| | | | 44.669 (15) | | | |
| 44.960 | 24 | | 44.832 (15) | | | 44.849 (22) |
| | | | 45.618 (20) | | | |
| 46.340 | 33 | | 45.740 (24) | | | 46.254 (26) |
| | | | | | 47.089 (35) | 47.859 (22) |
| 48.080 | 61 | | 48.008 (11) | 48.674 (16) | | 48.039 (27) |

**Table E.3:** Comparison of 2Θ values of peak points of C3 with standard 2Θ values of expected minerals with corresponding relative intensities

| Cement | | Possible cementitious minerals | | | | |
|---|---|---|---|---|---|---|
| C3 | | Yeelimite (33-0256) | Larnite (33-0302) | Anhydrite (37-1496 ) | Brownmillerite (30-0226 ) | Ternesite (49-1807) |
| 2Θ | R.I. | 2Θ (R.I.) | 2Θ (R.I.) | 2Θ (R.I.) | 2Θ (R.I.) | 2Θ (R.I.) |
| 19.500 | 14 | | 19.108 (9) | | 12.198 (45) | 19.389 (8) |
| 21.840 | 16 | | | | | |
| 22.600 | 24 | | | | | 22.494 (12) |
| 23.780 | 90 | 23.643(100) | | | 24.339 (16) | |
| 25.520 | 31 | | | 25.436(100) | | |
| 26.760 | 25 | | | | | 26.594 (17) |
| 28.000 | 49 | | | | | 27.874 (27) |
| 28.620 | 26 | | | | | 28.469 (14) |
| 29.440 | 33 | | 29.267 (9) | | | 29.334 (32) |
| 30.000 | 30 | | | | | 29.914 (11) |
| 30.480 | 19 | | 31.059 (21) | | | 31.324 (40) |
| 31.460 | 100 | | | 31.367 (29) | | 31.584(100) |
| | | | 31.773 (22) | | | |
| 31.660 | 83 | | 32.054 (97) | | | |
| | | | 32.136(100) | | 32.124 (25) | |
| | | | 32.593 (83) | | | |
| 32.700 | 19 | | 32.926 (30) | | | |
| 33.500 | 36 | | | | 33.497 (35) | |
| 33.840 | 37 | 33.796 (25) | | | 33.875 (100) | |
| 34.340 | 38 | | 34.330 (42) | | | 34.239 (32) |
| 35.020 | 55 | | | | 34.798 (17) | 34.949 (57) |
| 35.900 | 45 | | 35.235 (9) | | | |
| | | | 36.680 (12) | 38.640 (20) | | |
| | | | 37.280 (13) | | | |
| | | | 37.392 (18) | | | |
| 39.380 | 28 | | 39.473 (22) | | | 39.299 (22) |
| 40.860 | 19 | | | 40.815 (20) | | |
| 41.680 | 50 | 41.663 (20) | 41.206 (51) | | | 41.534 (17) |
| | | | 41.683 (13) | | | |
| 43.580 | 20 | | | 43.330 (8) | | |
| 43.940 | 18 | | 44.141 (14) | | 44.118 (35) | |
| | | | 44.669 (15) | | | |
| 44.940 | 24 | | 44.832 (15) | | | 44.849 (22) |
| | | | 45.618 (20) | | | |
| 46.320 | 31 | | 45.740 (24) | | | 46.254 (26) |
| | | | | | 47.089 (35) | 47.859 (22) |
| 48.060 | 47 | | 48.008 (11) | 48.674 (16) | | 48.039 (27) |

**Table E.4:** Comparison of 2Θ values of peak points of C4 with standard 2Θ values of expected minerals with corresponding relative intensities

| Cement | | Possible cementitious minerals | | | | |
|---|---|---|---|---|---|---|
| C4 | | Yeelimite (33-0256) | Larnite (33-0302) | Anhydrite (37-1496 ) | Brownmillerite (30-0226 ) | Ternesite (49-1807) |
| 2Θ | R.I. | 2Θ (R.I.) | 2Θ (R.I.) | 2Θ (R.I.) | 2Θ (R.I.) | 2Θ (R.I.) |
| 23.780 | 100 | 23.643(100) | | | 12.198 (45) | |
| 25.560 | 67 | | | 25.436(100) | 24.339 (16) | 27.874 (27) |
| | | | | | | 28.469 (14) |
| | | | | | | 29.334 (32) |
| 31.420 | 45 | | | 31.367 (29) | | 31.324 (40) |
| 32.600 | 52 | | 32.054 (97) | | | 31.584(100) |
| | | | 32.136(100) | | 32.124 (25) | |
| 32.920 | 65 | | 32.593 (83) | | | |
| 33.240 | 40 | | | | 33.497 (35) | |
| 33.660 | 49 | 33.796 (25) | | | 33.875 (100) | |
| | | | 34.330 (42) | | 34.798 (17) | 34.239 (32) |
| 35.880 | 44 | | 35.235 (9) | | | 34.949 (57) |
| 36.640 | 20 | | | | | |
| 38.740 | 15 | | 37.392 (18) | 38.640 (20) | | |
| 39.240 | 19 | | 39.473 (22) | | | 39.299 (22) |
| 40.840 | 30 | | | 40.815 (20) | | |
| 41.720 | 42 | 41.663 (20) | 41.206 (51) | | | |
| 43.560 | 23 | | | | 44.118 (35) | |
| | | | 45.618 (20) | | | 44.849 (22) |
| | | | 45.740 (24) | | | 46.254 (26) |
| 47.240 | 28 | | | | 47.089 (35) | |
| | | | | | | 47.859 (22) |
| 48.780 | 19 | | | 48.674 (16) | | 48.039 (27) |
| | | | | | 50.228 (45) | 50.474 (18) |
| 52.040 | 20 | | | 52.229 (11) | | 51.998 (21) |
| 52.360 | 22 | | | 52.289 (10) | | |
| 55.800 | 22 | | | 55.721 (15) | | |
| 56.660 | 23 | | 56.470 (12) | | | |
| 57.660 | 29 | | 57.400 (11) | | | |
| 58.540 | 23 | | | | 58.420 (14) | |
| 59.220 | 24 | | | | | |

**Table E.5:** Comparison of 2Θ values of peak points of C5 with standard 2Θ values of expected minerals with corresponding relative intensities

| Cement | | Possible cementitious minerals | | | | |
|---|---|---|---|---|---|---|
| C5 | | Yeelimite (33-0256) | Larnite (33-0302) | Anhydrite (37-1496 ) | Brownmillerite (30-0226 ) | Ternesite (49-1807) |
| 2Θ | R.I. | 2Θ (R.I.) | 2Θ (R.I.) | 2Θ (R.I.) | 2Θ (R.I.) | 2Θ (R.I.) |
| 23.760 | 100 | 23.643(100) | | | 12.198 (45) | |
| 25.520 | 57 | | | 25.436(100) | 24.339 (16) | 27.874 (27) |
| | | | | | | 28.469 (14) |
| | | | | | | 29.334 (32) |
| 31.380 | 31 | | | 31.367 (29) | | 31.324 (40) |
| 32.560 | 60 | | 32.054 (97) | | | 31.584(100) |
| | | | 32.136(100) | | 32.124 (25) | |
| 33.200 | 51 | | 32.593 (83) | | | |
| 33.380 | 39 | | | | 33.497 (35) | |
| 33.820 | 45 | 33.796 (25) | | | 33.875 (100) | |
| | | | 34.330 (42) | | 34.798 (17) | 34.239 (32) |
| 35.740 | 18 | | 35.235 (9) | | | 34.949 (57) |
| 36.600 | 18 | | 36.680 (12) | | | |
| 38.720 | 19 | | 37.392 (18) | 38.640 (20) | | |
| 39.240 | 16 | | 39.473 (22) | | | 39.299 (22) |
| 40.860 | 29 | | | 40.815 (20) | | |
| 41.700 | 43 | 41.663 (20) | 41.206 (51) | | | |
| 43.420 | 17 | | | | 44.118 (35) | 44.849 (22) |
| | | | 45.618 (20) | | | 46.254 (26) |
| | | | 45.740 (24) | | | |
| 46.840 | 19 | | | | 47.089 (35) | |
| 47.600 | 17 | | 48.008 (11) | | | 47.859 (22) |
| | | | | | | 48.039 (27) |
| 48.700 | 19 | | | 48.674 (16) | | |
| 50.640 | 13 | | | | 50.228 (45) | 50.474 (18) |
| 51.800 | 16 | | | 52.229 (11) | | 51.998 (21) |
| 52.320 | 17 | | | 52.289 (10) | | |
| 55.800 | 16 | | | 55.721 (15) | | |
| 56.660 | 16 | | 56.470 (12) | | | |
| 58.480 | 20 | | | | 58.420 (14) | |